Politecnico di Milano

On the intra-granular behaviour of a cocktail of helium and fission gas in oxide nuclear fuel

Supervisor
Davide PIZZOCRI

Co-Supervisor
Lelio LUZZI

Candidate
Mariagrazia ROMANO – 927945

Aknowledgements

Contents

List of Acronyms

BC Boundary Condition

EOS Equation Of State

FG Fission Gas

FGR Fission Gas Release

FPC Fuel Performance Code

IGB Inert Gas Behaviour

PCMI Pellet-Cladding Mechanical Interaction

TEM Transmission Electron Microscopy

List of Symbols

β	helium trapping rate	s^{-1}
$\dot{F}$	Fission rate density	$\text{fiss m}^{-3}\text{ s}^{-1}$
γ	thermal re-solution rate	s^{-1}
μ_{ff}	average length of a fission spike	m
ν_{het}	heterogeneous nucleation rate	$\text{nucleated bubbles m}^{-3}\text{ s}^{-1}$
ν_{hom}	homogeneous nucleation rate	$\text{nucleated dimers m}^{-3}\text{ s}^{-1}$
a	grain radius	m
b	irradiation induced re-solution rate	s^{-1}
b'	homogeneous re-solution rate	s^{-1}
b''	heterogeneous re-solution rate	s^{-1}
c	gas grain solution concentration	at m^{-3}
$C_{S,He}$	helium solubility	at m^{-3}
D	Diffusion coefficient	$\text{m}^2\text{ s}^{-1}$
d	hard sphere diameter	m
g	trapping rate	s^{-1}
g'	bubbles trapping rate	$\text{m}^3\text{ bubble}^{-1}\text{ s}^{-1}$
k_B	Boltzmann's constant	J K^{-1}
k_H	Henry's constant	$\text{at m}^{-3}\text{ MPa}^{-1}$
M	mass	g
m	gas grain bubbles concentration	at m^{-3}
M_M	molar mass	g mol^{-1}
n	atoms per intra-granular bubbles	at bubble^{-1}

N_{av}	Avogadro's number	at mol^{-1}
N_{ig}	intra-granular bubble density	bubbles m^{-3}
p	pressure	MPa
R_{at}	atomic radius	m
R_{ff}	average radius of a fission spike	m
R_{ig}	intra-granular bubble radius	m
S	atoms source rate	at m^{-3} s^{-1}
T	Temperature	K
t	time	s
V_{at}	atomic volume	m^3
V_{ig}	intra-granular bubble volume	m^3
w	weight factor	—
$w_{\%}$	weight percentage	—
x	mole fraction of a gas	—
y	volumetric fraction of a gas	—
y_F	fission yield	—
Z	compressibility factor	—

List of Figures

List of Tables

Abstract

The description of intra-granular gas behaviour is typically a first part of models for the prediction of gas release and swelling in nuclear fuel performance codes. The state-of-art modelling resorts to independent models to describe the behaviour of helium and fission gases (xenon and krypton) in the fuel grain. This thesis represents a first attempt to address their coupled intra-granular behaviour. It is proposed a model that results from the evolution of intra-granular bubble population through the physical processes of single gas atom diffusion, gas bubble nucleation, irradiation induced and thermal re-solution and gas atom trapping at bubbles. The model is implemented in SCIANTIX, an open source 0D stand-alone computer code designed to be coupled/included in fuel performance codes. As a result of the work done, SCIANTIX can handle the coupled as well as the independent intra-granular inert gas models. An experimental program investigating the behaviour of inert gas cocktails in annealing conditions is planned in the frame of different research initiatives. Due to the lack of experimental data necessary for the model validation, several annealing scenarios are reproduced. These simulations lay the foundation for future experimental investigations on cocktails of inert gases. The aim is to produce the basis for targeted experiments considering the proposed results. They enable to identify suitable ranges of temperature, gas compositions in the grain and gas fractional release in which the model predicts an observable interaction between helium and fission gas. The massive presence of helium in the cocktail influences the fission gas release to such an extent that their interaction cannot be neglected. To further support the annealing simulations, it is performed a sensitivity analysis with the Pareto method quantifying the impact of the uncertainties in four model parameters on the model behaviour. The sensitivity analysis points out that the diffusion coefficients and Henry's constant have the major influence on the model behaviour prioritising the reduction of their uncertainties to improve the model predictive capability.

Sommario

La descrizione del comportamento intra-granulare dei gas è tipicamente una delle prime fasi nella realizzazione di modelli che prevedono il rilascio di gas e il rigonfiamento del combustibile nucleare nei codici di *performance*. Allo stato dell'arte si ricorre a modelli indipendenti per descrivere il comportamento di elio e gas di fissione (xenon e krypton) nel grano di combustibile. Questa tesi rappresenta un primo tentativo di affrontare il loro comportamento accoppiato. Viene presentato un modello risultante dall'evoluzione della popolazione di bolle intra-granulari attraverso i processi fisici di diffusione degli atomi singoli, nucleazione di bolle, risoluzione indotta dall'irraggiamento e termica e assorbimento degli atomi alle bolle. Il modello è implementato in SCIANTIX, un codice progettato per essere accoppiato/incluso nei codici di *performance*. Come risultato del lavoro svolto SCIANTIX può ricorrere al modello intra-granulare accoppiato così come ai modelli indipendenti dei gas inerti. Un programma sperimentale che esplora il comportamento dei *cocktail* di gas in condizioni di *annealing* è previsto da parte di diverse attività di ricerca. In un'ottica di sinergia tra modellazione ed esperimenti si applica il nuovo modello alla simulazione di molteplici scenari di *annealing*. Le simulazioni suggeriscono le basi di partenza per la messa a punto di futuri esperimenti sui *cocktail* di gas inerti. Esse permettono infatti di identificare intervalli di temperatura e di composizioni gassose nel grano in cui il modello prevede un'interazione osservabile tra elio e gas di fissione. L'alta quantità di elio nel *cocktail* influenza il rilascio dei gas di fissione al punto tale da non poter trascurare una loro reciproca influenza. Come ulteriore supporto alle simulazioni, un'analisi di sensitività che sfrutta il metodo di Pareto quantifica l'impatto delle incertezze di quattro parametri sul comportamento del modello. L'analisi evidenzia che i coefficienti di diffusione e la costante di Henry hanno la maggiore influenza, sottolineando la priorità nella riduzione delle loro incertezze per migliorare la capacità predittiva del modello.

Estratto in italiano

Introduzione

Il rigonfiamento del combustibile (*swelling*) e il rilascio di gas giocano un ruolo fondamentale nel determinare il comportamento termo-meccanico delle barre di combustibile nucleare in condizioni di irraggiamento. Per tale motivo, i modelli che simulano il comportamento intra-granulare dei gas risultano essenziali nei codici di *performance* del combustibile nucleare. Il lavoro di tesi si focalizza su elio, xenon e krypton. Allo stato dell'arte la descrizione dei gas inerti è affrontata attraverso modelli indipendenti, ovvero producendo modelli separati per elio e gas di fissione. Non viene descritta una loro interazione nel grano che potrebbe avere riscontri sulle prestazioni del combustibile. Questa tesi rappresenta un primo tentativo di riprodurre il loro comportamento accoppiato attraverso un modello che delinea l'evoluzione di bolle intra-granulari miste (contenenti elio e gas di fissione) nel combustibile ossido. ll modello è implementato in SCIANTIX, un codice che descrive il comportamento dei gas all'interno del combustibile. Sono successivamente riprodotti diversi scenari di *annealing* con lo scopo di proporre le basi per la progettazione di futuri esperimenti sui gas inerti. Le simulazioni mostrano un'interazione dei gas all'interno delle bolle, avvalorando l'importanza del loro accoppiamento. Un'analisi di sensitività infine evidenzia i coefficienti di diffusione e la costante di Henry come i parametri la cui incertezza ha un maggior impatto sul modello in condizioni di *annealing*.

Di seguito vengono elencate le principali tappe del lavoro svolto.

1. Sviluppo di un modello fisico che descrive il comportamento intra-granulare accoppiato di un *cocktail* di gas inerti composto da elio e gas di fissione. Il sistema di equazioni proposto si basa sui processi fisici di diffusione degli atomi di gas, nucleazione delle bolle, risoluzione dalle bolle al reticolo ed assorbimento degli atomi singoli da parte delle bolle.

2. Implementazione del modello in SCIANTIX, un codice che descrive il comportamento dei gas di fissione all'interno del combustibile nucleare. Il codice lavora in modo indipendente ma può anche essere adottato come modulo da includere all'interno dei codici di *performance* del combustibile. Come risultato del lavoro svolto, SCIANTIX è in grado di gestire sia la descrizione dei gas inerti attraverso modelli separati per elio e gas di fissione sia il loro comportamento misto attraverso un unico modello.

3. Attraverso una versione ridotta del modello sono stati simulati diversi sce-

nari di *annealing*. Queste simulazioni mirano allo sviluppo futuro del modello, perché il loro intento è quello di suggerire esperimenti che permettano di ottenere i dati più utili alla sua validazione. La scelta nasce dal fatto che sono in programma diverse iniziative di ricerca a riguardo. Lo scopo è quello di individuare quali siano gli intervalli più promettenti da investigare in termini di temperatura o di combinazioni gassose per osservare un'interazione tra i gas. Si considerano i casi di *annealing* perché corrispondono alle condizioni sperimentali più comode da realizzare e più semplici da riprodurre, soprattutto ai primi stadi di sviluppo del modello proposto.

4. Infine è proposta un'analisi di sensitività, che attraverso il metodo di Pareto analizza quattro parametri significativi per le simulazioni di *annealing*. L'obiettivo è determinare quale sia il parametro la cui incertezza abbia un peso maggiore sul modello. I risultati servono a supportare le osservazioni sulle simulazioni di *annealing* ma soprattutto evidenziano qual è il parametro il cui miglioramento sperimentale ha la priorità nello sviluppo delle capacità predittive del modello. Quest'analisi serve anche a limitare gli sforzi di futuri esperimenti in termini di tempo e risorse.

Processi intra-granulari

La descrizione dei processi fisici che controllano la formazione e l'evoluzione delle bolle intra-granulari nel combustibile pone le basi del modello proposto. Ogni processo viene introdotto tramite un parametro che dipende dal tipo di gas considerato (elio o gas di fissione).

Diffusione. Il primo processo che avviene dopo la produzione degli atomi di gas è la diffusione degli stessi all'interno del reticolo. Nel loro percorso gli atomi possono raggiungere il bordo grano e venire rilasciati. La diffusività dell'elio all'interno del combustibile ossido è maggiore rispetto a quella di xenon e krypton, a tal proposito si utilizzano due formulazioni differenti. Il modello non contempla la diffusione delle bolle, assumendo che queste siano immobili [47].

Il coefficiente di diffusione D_{He} (m^2 s^{-1}) per l'elio proviene dal lavoro di Luzzi et al. [17] ed è raccomandato per campioni infusi con danneggiamento del reticolo limitato o nullo:

$$D_{He} = 2 \times 10^{-10} \exp\left(\frac{-2.12 \text{ eV}}{k_B T}\right) \tag{1}$$

dove k_B (J K^{-1}) è la costante di Boltzmann e T (K) la temperatura.

Per quanto riguarda i gas di fissione, Turnbull [41] propone la seguente espressione per il coefficiente di diffusione D_{FG} (m^2 s^{-1}), in funzione di temperatura, stechiometria e tasso di fissione:

$$
\begin{aligned}
D &= D_1 + D_2 + D_3 \\
D_1 &= 7.6 \times 10^{-10} \exp\left(-4.86 \times 10^{-19}/k_B T\right) \\
D_2 &= 5.64 \times 10^{-25} \sqrt{\dot{F}} \exp\left(-1.91 \times 10^{-19}/k_B T\right) \\
D_3 &= 2.0 \times 10^{-40} \dot{F}
\end{aligned}
\tag{2}
$$

D_1 dipende dalla temperatura del combustibile e domina oltre i 1400°C, D_2 dipende dalla temperatura del combustibile ma anche dal tasso di fissione ($\dot{F}$) e domina quando 1000°C < T < 1400°C, D_3 è la componente atermica e prevale sotto i 250°C [44].

Nucleazione. Il processo di nucleazione si riferisce alla formazione delle bolle. Olander [27] distingue due differenti meccanismi di nuclezione che agiscono all'interno del grano, meccanismo omogeneo ed eterogeneo.

La nucleazione eterogenea consiste nella creazione di bolle come risultato dell'interazione tra i frammenti di fissione ed il reticolo. I frammenti di fissione lasciano lungo il loro percorso agglomerati di vacanze che costituiranno i nuclei delle nuove bolle. Il modello presentato considera solamente la nucleazione eterogenea nelle sue equazioni, poichè risulta dominare nei combustibili ossidi. Il tasso di nucleazione eterogenea (bolle nucleate m^{-3} s^{-1}) è il seguente:

$$\nu_{het} = 2\dot{F}\alpha \tag{3}$$

Il fattore 2 considera il numero di frammenti prodotti per fissione, $\dot{F}$ è il tasso di fissione (fissioni m^{-3} s^{-1}) e α corrisponde al numero di bolle nucleate da ogni frammento di fissione.

Il meccanismo omogeneo si riferisce alla nucleazione di bolle per effetto della diffusione degli atomi dissolti nel reticolo. Olander [27] fornisce una descrizione molto più dettagliata di questi meccanismi.

Risoluzione. Il continuo flusso di atomi di gas tra le bolle ed il reticolo richiede l'introduzione nel modello del termine di risoluzione. La risoluzione è distinta in due classi a seconda del meccanismo trainante, risoluzione indotta dai frammenti di fissione e risoluzione termica.

Per quanto riguarda la risoluzione indotta dai framenti di fissione, Olander [27] applica la stessa distinzione tra meccanismo eterogeneo ed omogeneo utilizzata per la nucleazione. La risoluzione eterogenea consiste nella distruzione in blocco delle bolle ad opera dei frammenti di fissione. Il tasso di risoluzione eterogenea può essere definito come:

$$b_{het} = \frac{bolle\ dissolte}{bolle - unità\ di\ tempo} \tag{4}$$

Le risoluzione omogenea invece consiste nell'espulsione graduale degli atomi dalle bolle per effetto di collisioni con i frammenti di fissione. Quest'ultima viene espressa come:

$$b_{hom} = \frac{atomi\ dissolti}{atomi - unità\ di\ tempo} \tag{5}$$

Il reciproco di questo termine è il tempo medio che un atomo trascorre in una bolla. La peculiarità dell'elio consiste nella sua più alta solubilità in confronto a xenon e krypton, la cui solubilità è generalmente trascurata [16]. A tal proposito si richiede di introdurre nel modello la definizione di risoluzione termica. La solubilità è espressa in funzione di pressione e temperatura (tramite la costante di Henry) come segue:

$$C_{S,He}(\text{at m}^{-3}) = k_H p \tag{6}$$

dove k_H (at m^{-3} MPa^{-1}) è la costante di Henry e p (MPa) è la pressione parziale dell'elio nelle bolle intra-granulari. Si assume che la legge di Henry sia valida nel sistema He-UO$_2$ come verificato da un seppur piccolo set di dati sperimentali [36]. Per la definizione della costante di Henry si fa riferimento alla formula proposta da Cognini et al.[8] valida per cristalli singoli nell'intervallo di temperatura di 1073-1773 K:

$$k_H = 4.1 \times 10^{24} \exp\left(\frac{-0.65 \text{ eV}}{k_B T}\right) \tag{7}$$

dove k_B (J K^{-1}) è la costante di Boltzmann and T (K) la temperatura. In conclusione, la risoluzione termica è espressa dalla formula $\beta k_H p$, dove β corrisponde al tasso di assorbimento di Ham [14]. Questa formulazione verrà approfondita nella sezione successiva, in cui si spiega la struttura del modello.

Assorbimento. La taglia delle bolle aumenta per assorbimento degli atomi di gas durante la loro diffusione. Il tasso di assorbimento corrisponde a:

$$g = \frac{atomi \; assorbiti}{atomi - unità \; di \; tempo} \tag{8}$$

Nel modello si utilizza la formulazione derivata da Ham [14].

Raggio della bolla. Viene infine dato risalto alla formulazione del raggio delle bolle, poichè identifica il ponte di collegamento tra i diversi atomi all'interno del modello. Il raggio infatti considera la coesistenza di elio e gas di fissione nelle bolle. Assumendo che le bolle intra-granulari siano sferiche, il volume della singola bolla (m^3) è dato da:

$$V_{ig} = n_{He} V_{He} + n_{FG} V_{FG} = \frac{4}{3}\pi R_{ig}^3 \tag{9}$$

Invertendo l'equazione si ricava il raggio della bolla (m):

$$R_{ig} = \left[\frac{3}{4\pi}(n_{He} V_{He} + n_{FG} V_{FG})\right]^{1/3} \tag{10}$$

dove n (at bubble^{-1}) è differente tra elio e gas di fissione. V_{He} è il volume atomico dell'elio corrispondente a 7.8×10^{-30} m^3 [7]. Per i gas di fissione il volume atomico nelle bolle è 4.09×10^{-29} m^3, uguale al volume del difetto di Schottky [15].

Modello fisico

Modello matematico. Il modello proposto descrive il comportamento intra-granulare accoppiato di un *cocktail* di gas inerti nello specifico elio, xenon e krypton. Nella sua forma finale è costituito da sette equazioni differenziali, tre delle quali si riferiscono ai gas di fissione, tre all'elio e l'ultima al numero di bolle. Per la formulazione del sistema di equazioni si è fatto riferimento al lavoro di Cognini et al. [7] sull'elio, mentre per quanto riguarda i gas di fissione il lavoro di riferimento è quello di Pizzocri et al. [30]. Si ricorda infatti che il modello rappresenta un primo passo verso l'accoppiamento tra elio e gas di fissione nel grano, la cui descrizione allo

stato dell'arte è affrontata attraverso modelli indipendenti. Di seguito è riportato il sistema che è stato implementato in SCIANTIX.

Gas di fissione

$$\frac{\partial c_{FG}}{\partial t} = S_{FG} + D_{FG}\nabla^2 c_{FG} - g_{FG}c_{FG} + b_{FG}m_{FG} - \nu n_{FG} \tag{11}$$

$$\frac{\partial m_{FG}}{\partial t} = g_{FG}c_{FG} - b_{FG}m_{FG} + \nu n_{FG} \tag{12}$$

$$\frac{\partial n_{FG}}{\partial t} = g'_{FG}c_{FG} - b'_{FG}n_{FG} \tag{13}$$

Elio

$$\frac{\partial c_{He}}{\partial t} = S_{He} + D_{He}\nabla^2 c_{He} - g_{He}c_{He} + b_{He}m_{He} + \gamma m_{He} - \nu n_{He} \tag{14}$$

$$\frac{\partial m_{He}}{\partial t} = g_{He}c_{He} - b_{He}m_{He} - \gamma m_{He} + \nu n_{He} \tag{15}$$

$$\frac{\partial n_{He}}{\partial t} = g'_{He}c_{He} - b'_{He}n_{He} - \gamma n_{He} \tag{16}$$

Numero di bolle

$$\frac{\partial N}{\partial t} = \nu - b''N \tag{17}$$

Le variabili principali sono: c la concentrazione di gas in soluzione (at m^{-3}), m la concentrazione di gas nelle bolle del grano (at m^{-3}), n atomi per bolle intragranulari (at bolla^{-1}) e N la densità di bolle (bolle m^{-3}). I pedici identificano gas di fissione (FG) ed elio (He). S è il tasso di generazione degli atomi (at m^{-3} s^{-1}), γ è la risoluzione termica (s^{-1}). Considerando le bolle, g' corrisponde a $\frac{g}{N}$ ed è il tasso di assorbimento delle bolle (m^3 bolle^{-1} s^{-1}). b' e b'' rappresentano il tasso di risoluzione omogenea ed eterogenea (s^{-1}) rispettivamente.
La popolazione delle bolle è descritta da un modello a taglia singola. Le bolle nascono ad una taglia media e sempre ad una taglia media vengono distrutte attraverso il meccanismo di risoluzione eterogenea. Tale assunzione è supportata da osservazioni TEM che asseriscono che i raggi delle bolle siano confinati a intervalli ristretti [27]. Le condizioni iniziali per c, m, n, N ed il raggio del grano a possono essere introdotte come input esterni nel codice SCIANTIX.
Considerando il problema della diffusione degli atomi singoli si assumono le stesse condizioni al contorno per elio e gas di fissione:

$$c(a) = 0 \tag{18}$$

$$\left(\frac{\partial c}{\partial r}\right)_{r=0} = 0 \tag{19}$$

La prima equazione assume che il bordo grano agisca come un pozzo per gli atomi che diffondono, ovvero una volta raggiunto il bordo grano gli atomi non possono più rientrare. La seconda equazione implica una simmetria nella concentrazione del gas nel grano.

Meccanismi di risoluzione indotta dall'irraggiamento. Il modello in questione comprende sia la risoluzione omogenea che eterogenea attraverso i parametri b' e b''. Per far ciò, si introduce una terna di fattori di peso (w_{He}, w_{FG} e w_N) che permette la conservazione del parametro di risoluzione totale b (s^{-1}). Tale parametro si esprime come contributo della risoluzione omogenea dell'elio (b'_{He}), dei gas di fissione (b'_{FG}) e della risoluzione eterogenea (b'') comune a entrambi i tipi di gas poichè sono contemporaneamente presenti nelle bolle.

$$b = b'_{He} + b'_{FG} + b'' \tag{20}$$

dove

$$
\begin{aligned}
b'_{He} &= w_{He}b \\
b'_{FG} &= w_{FG}b \\
b'' &= w_N b
\end{aligned}
\tag{21}
$$

Dalle precedenti equazioni si deriva la formulazione che lega proporzionalmente i fattori di peso:

$$1 = w_{He} + w_{FG} + w_N \tag{22}$$

Attraverso questa equazione viene mantenuta la proporzionalità tra i meccanismi di risoluzione e tra le variabili m, n e N, ricordando che $m = nN$. Le bolle di puro elio o puro gas di fissione sono tenute in considerazione ponendo w_{He} o w_{FG} uguale a uno. I valori associati ai fattori di peso sono arbitrari, poichè non ci sono riferimenti in letteratura a riguardo. Uno studio più approfondito potrebbe risultare di interesse in prospettiva.

Equazione di stato e risoluzione termica. La solubilità dell'elio (Eq.6) richiede di valutare la pressione del gas nelle bolle intra-granulari. Risulta perciò necessario identificare un'equazione di stato. Poichè le bolle sono formate da differenti specie atomiche, si assume che la pressione esercitata dall'elio sia una pressione parziale. Secondo la legge di Dalton delle pressioni parziali risulta che la pressione totale (Pa) a cui è sottoposta la bolla sia data dalla somma di due contributi:

$$p_{ig} = p_{FG} + p_{He} \tag{23}$$

Ricordando che tale legge può essere espressa anche attraverso la frazione molare (x) e adottando la formula di Carnahan–Starling [5] che lega la pressione della bolla alla temperatura e al volume dei gas, si ottiene:

$$p_{He} = x_{He}p_{ig} = \frac{n_{He}}{n_{tot}}\left(\frac{k_B T Z}{V_{ig}}n_{tot}\right) = \frac{k_B T Z}{V_{ig}}n_{He} \tag{24}$$

dove n è il numero di atomi per bolla, k_B (J K^{-1}) è la costante di Boltzmann, T (K) la temperatura, V_{ig} è il volume della bolla (m^3) e Z il fattore di comprimibilità. Quest'ultimo fattore indica la deviazione dei gas dal comportamento ideale e viene ricavato attraverso il diametro di sfera rigida introdotto da Van Brutzel [42].
Per completare lo studio della solubilità, si ricava infine la risoluzione termica. Nel modello viene dedotta dal prodotto tra il tasso di assorbimento dell'elio β e la sua solubilità nel seguente modo:

$$\beta k_H p_{He} = (4\pi D_{He} R_{ig} N_{ig})\, k_H \left(\frac{k_B T Z}{V_{ig}}n_{He}\right) = \gamma\,(n_{He}N_{ig}) \tag{25}$$

dove D_{He} è il coefficiente di diffusione dell'elio (m^2 s^{-1}), R_{ig} è il raggio della bolla (m), k_H è la costante di Henry (at m^{-3} MPa^{-1}) e N_{ig} è la densità di bolle (bolle m^{-3}). La formula della risoluzione termica (s^{-1}) che rientra nel modello risulta essere:

$$\gamma = 4\pi R_{ig} D_{He} k_H \frac{k_B T Z}{V_{ig}} \tag{26}$$

Comportamento del modello in condizioni di *annealing*

Come già menzionato nell'introduzione, la mancanza di dati sperimentali ha impedito la validazione del modello. Vengono perciò proposte diverse simulazioni di *annealing* che permettono di analizzare il modello e anticipano futuri esperimenti sui *cocktail* di gas inerti programmati in diverse attività di ricerca. Le simulazioni pongono le basi per poter realizzare degli esperimenti mirati ad osservare un'interazione tra i gas nel grano. Le storie di *annealing* riprodotte richiedono una versione ridotta del modello che considera solamente i processi di diffusione, risoluzione termica e assorbimento. Ogni storia è caratterizzata da una rampa di riscaldamento seguita dal mantenimento della stessa temperatura per 20 ore. L'intervallo di temperature analizzato va dai 1000 K ai 2000 K, per poter includere la maggior parte delle temperature operative del combustibile in reattore. Le quantità iniziali di gas di fissione nel grano sono determinate partendo da due casi di irraggiamento, a basso burn-up (circa 240 MWd/t$_U$) e ad alto burn-up (circa 100 GWd/t$_U$). I valori scelti corrispondono ai periodi di irraggiamento di interesse per quanto riguarda i gas di fissione nei reattori veloci, ovvero ad inizio vita a valle della ristrutturazione del combustibile e a fine vita. Il valore di alto burn-up corrisponde ad un limite superiore per i reattori veloci. La quantità iniziale di elio (M_{He}) è ottenuta variando la sua percentuale in peso ($w_{\%He}$) rispetto alla massa totale dei gas di fissione (M_{FG}):

$$M_{He} \text{ (g)} = \frac{w_{\%He}}{1 - w_{\%He}} M_{FG} \tag{27}$$

La percentuale in peso permette di considerare gli effetti dovuti alle diverse dimensioni degli atomi. La figura di merito analizzata alla fine di ogni simulazione in SCIANTIX è il rilascio frazionario di gas a bordo grano. I risultati sono raccolti in grafici tridimensionali al variare della temperatura di *annealing* e della percentuale in peso di ogni componente del *cocktail* (Fig.1−4).

Simulazioni a basso burn-up. Come atteso il rilascio di elio aumenta con la temperatura fino al rilascio completo alle temperature più alte (Fig. 1). Ciò implica che tutti gli atomi di elio intrappolati nelle bolle abbiano subito risoluzione termica seguita dalla diffusione fino al bordo grano. Il gradiente di rilascio indica un'iniziale prevalenza del processo di assorbimento alle bolle incalzato ad alte temperature da diffusione e risoluzione. La grande differenza tra elio e gas di fissione nella quantità di atomi rilasciati a bordo grano è associata al fatto che xenon e krypton non sono soggetti alla risoluzione termica, ovvero una volta assorbiti dalle bolle vi rimangono bloccati senza poter rientrare in soluzione, in accordo con la versione ridotta

del modello. La diffusione è l'unico processo per cui possono raggiungere il bordo grano. Ciò è vero sia a basso che ad alto burn-up. Inoltre si nota come nel grafico dei gas di fissione (Fig. 2) il rilascio massimo sia limitato ad un intervallo di temperature ristretto che non include le temperature massime. In modo controintuitivo, il rilascio dei gas prima dei 2000 K torna a diminuire dovuto ad un effetto alternato tra i processi di assorbimento e diffusione. Per concludere, il rilascio frazionario di gas di fissione decresce proporzionalmente alla percentuale di gas nel *cocktail*, in modo complementare il rilascio di elio aumenta con la sua percentuale. Il modello predice quindi un'interazione tra gli atomi all'interno delle bolle. L'effetto diventa sempre più evidente all'aumentare della quantità di elio, che promuove l'assorbimento dei gas di fissione piuttosto che la loro diffusione a bordo grano.

Figure 1: Rilascio frazionario dell'elio a basso burn-up (240 MWd/t_U).
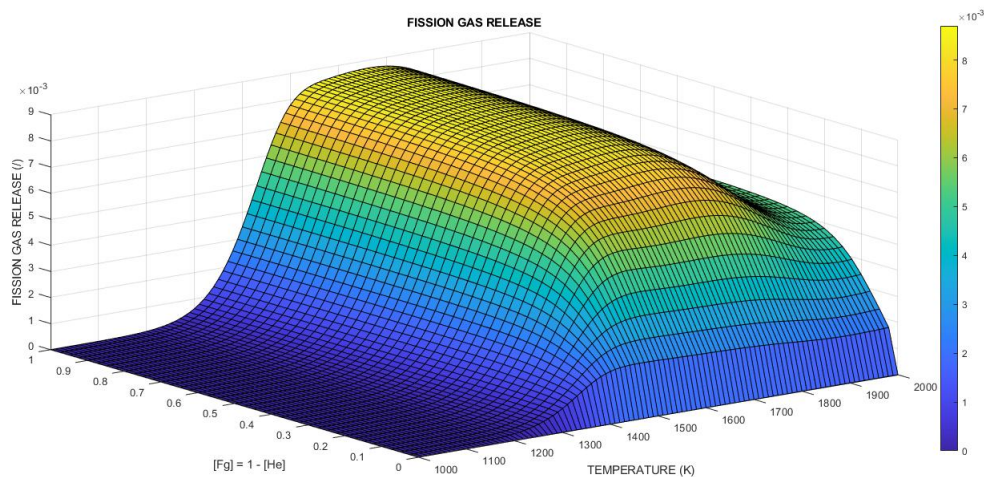
Figure 2: Rilascio frazionario dei gas di fissione a basso burn-up (240 MWd/t_U).

Simulazioni ad alto burn-up. La quantità di gas prodotta nelle simulazioni di alto burn-up è maggiore rispetto al caso precedente. Ciò farebbe pensare di poter avere più rilascio a bordo grano, ma in realtà i grafici 3 e 4 mostrano un rilascio inferiore sia per elio che per gas di fissione rispetto al caso di basso burn-up. Nonostante le alte temperature, il modello non prevede grandi rilasci con concentrazioni così alte di gas, specialmente se il *cocktail* è in prevalenza formato da elio. I processi di diffusione e di risoluzione termica hanno un effetto evidente sull'elio solamente a basse percentuali in peso e ad alte temperature. Il processo di assorbimento prevale per gran parte dei grafici riferiti ad elio e gas di fissione. Vale a dire che gli atomi in soluzione nel loro percorso verso il bordo grano hanno più possibilità di essere assorbiti alle bolle piuttosto che essere rilasciati. L'interazione fra i gas si nota a tutte le combinazioni di gas nel *cocktail*, il motivo è associato alle grandi quantità di atomi nel grano.
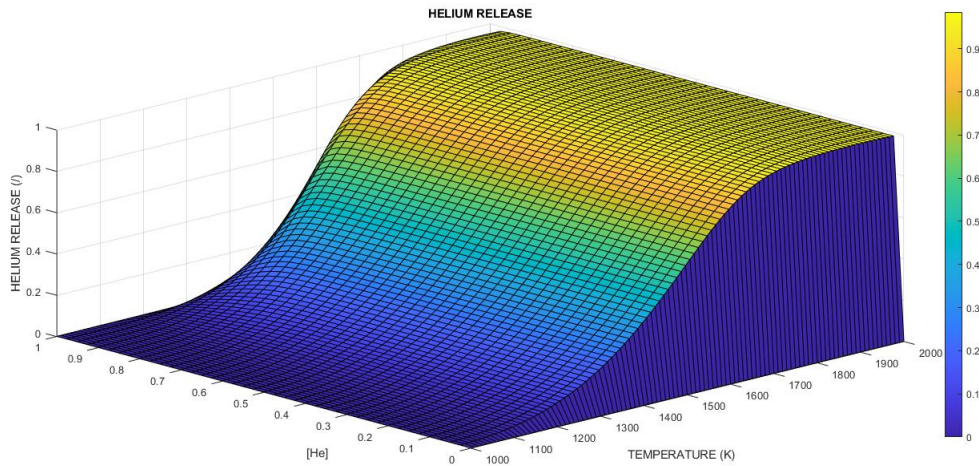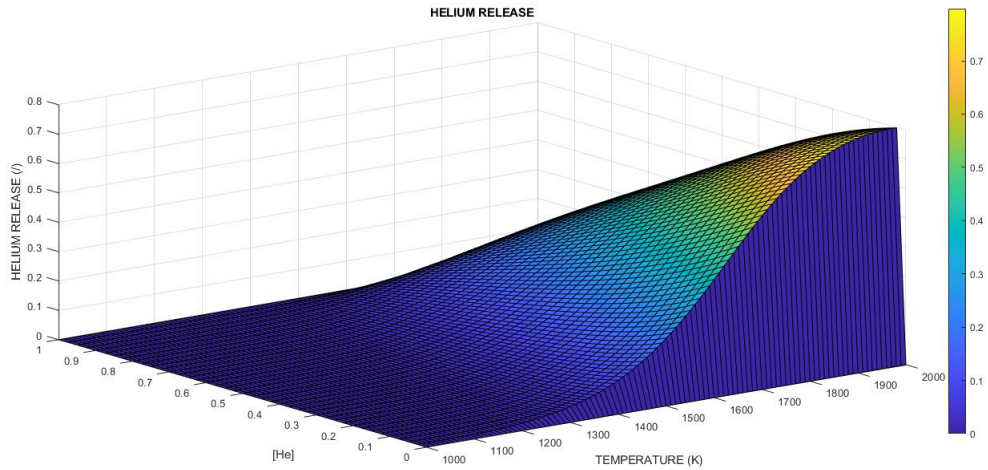
Figure 3: Rilascio frazionario dell'elio ad alto burn-up (100 GWd/t$_{\text{U}}$).
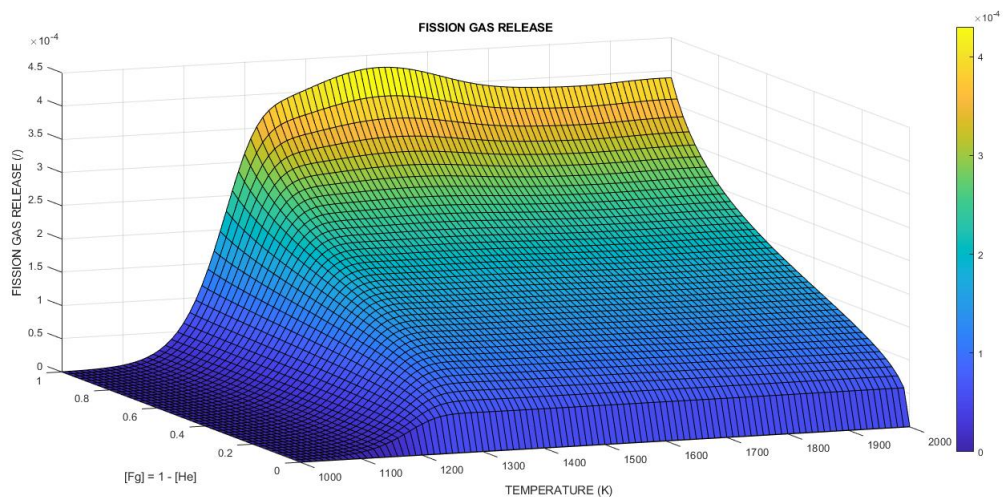
Figure 4: Rilascio frazionario dei gas di fissione ad alto burn-up (100 GWd/t$_{\text{U}}$).

Discussione dei risultati. Le simulazioni permettono di individuare intervalli di temperatura, combinazioni gassose del *cocktail* e rilasci di gas che potrebbero servire come punti di partenza per la progettazione di futuri esperimenti sui gas inerti. Il modello predice un'effettiva interazione tra i gas all'interno del grano.

In figura 5 vengono suggeriti i possibili intervalli di esplorazione. Considerando le linee a sinistra, a basso burn-up si suggerisce un *cocktail* formato al 50% da elio. Questa combinazione permette di osservare il gradiente di rilascio al variare della temperatura, identificando l'insorgere della diffusione. I rettangoli sempre nella zona di basso burn-up mettono in luce la combinazione di gas in cui è evidente un'interazione, perché la quantità di elio è alta. Gli stessi rettangoli coprono le zone di massimo rilascio per sottolineare il peso relativo dell'assorbimento rispetto a diffusione e risoluzione termica. Nel grafico dei gas di fissione viene coperta anche la discesa del rilascio alle alte temperature.

Ad alto burn-up il rilascio di elio e gas di fissione cambia continuamente con la percentuale in peso, quindi l'intero intervallo di combinazioni sarebbe interessante. Le linee diagonali evidenziano il gradiente di rilascio e le regioni di massimo rilascio atteso, che risulta limitato ad alte temperature e basse percentuali in peso di elio. Il processo di assorbimento ha infatti un peso relativo maggiore sulle simulazioni. L'ultimo rettangolo sulla destra sottolinea che, nonostante le alte temperature, il rilascio atteso non è molto alto. Suggerisce inoltre di approfondire il comportamento dei gas quando una grande quantità di elio è presente nel *cocktail*, perché è osservabile un'interazione significativa.
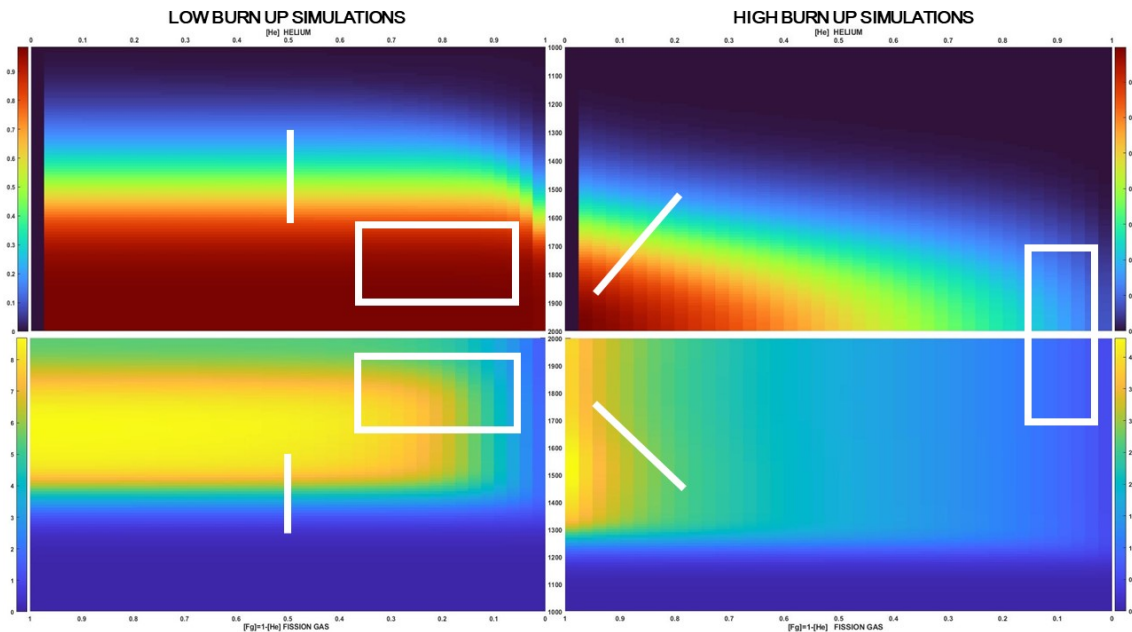
Figure 5: Vista specchiata delle simulazioni a basso ed alto burn-up. Le linee bianche evidenziano gli intervalli di ricerca suggeriti. Le barre di colore sull'esterno indicano il rilascio frazionario di gas. L'asse superiore ed inferiore indicano rispettivamente le percentuali in peso di elio e gas di fissione. L'asse verticale al centro corrisponde alla temperatura.

Analisi di sensitività

A completamento delle simulazioni di *annealing* è stata condotta un'analisi di sensitività su quattro parametri del modello facendo ricorso al metodo di Pareto. L'analisi permette di identificare il parametro la cui incertezza ha l'impatto maggiore sul modello. Lo scopo è di incoraggiare nuovi esperimenti mirati a ridurre l'incertezza dei parametri più significativi al fine di migliorare la capacità predittiva del modello sia in caso di *annealing* che in caso di irraggiamento. Considerando il numero limitato di processi fisici coinvolti nelle simulazioni, i parametri scelti corrispondono a: coefficiente di diffusione dell'elio e dei gas di fissione (D_{He}, D_{FG}), costante di Henry (k_H) e fattore di comprimibilità (Z). L'intervallo di incertezza associato ad ogni parametro viene simulato ricorrendo a dei fattori di scala riportati in tabella 1. Nel riprodurre le simulazioni di *annealing* per ogni intervallo di incertezza viene mantenuta la stessa distinzione tra alto e basso burn-up. La metrica di confronto riportata sui grafici di Pareto si basa sulla variazione del rilascio frazionario di gas dovuta all'incertezza associata al parametro in esame.

Dalle simulazioni di basso burn-up (Fig.6) emerge che il coefficiente di diffusione ha il peso maggiore sul modello sia nel caso dell'elio sia nel caso dei gas di fissione, seguito dalla costante di Henry. Questo risultato era atteso dato che il coefficiente di diffusione è alla base di tutti i processi in gioco. Dai grafici tridimensionali infatti si nota come l'assorbimento prevalga a basse temperature mentre diffusione e risoluzione termica intervengano a temperature più alte. Tutti i processi infatti contengono il coefficiente di diffusione. Il peso della costante di Henry è associato al suo ampio intervallo di incertezza. Si sottolinea il fatto che la costante di Henry abbia un peso non completamente trascurabile anche sul rilascio dei gas di fissione. La risoluzione termica influisce sul raggio delle bolle e si suppone che attraverso di questo abbia conseguenze indirette sui gas di fissione.

Ad alto burn-up (Fig.7) ci si aspetterebbe un comportamento simile poichè è il processo di assorbimento a dominare nei grafici di *annealing*. In realtà la costante di Henry risulta il parametro dominante nel caso dell'elio ed assume un peso maggiore anche per i gas di fissione. Considerando la grande quantità di atomi intrappolati nelle bolle, si assume che la variazione nella risoluzione termica (legata alla costante di Henry) abbia un effetto maggiore rispetto al caso di basso burn-up. In altre parole, la bassa quantità di elio rilasciato a bordo grano è fortemente influenzata dall'ampia variazione della costante di Henry. Il coefficiente di diffusione per i gas di fissione ha sempre il primo posto come previsto. In entrambi i casi di burn-up analizzati il fattore di comprimibilità risulta avere conseguenze trascurabili sul modello. Questo

Table 1: Fattori di scala per l'analisi di Pareto

Simbolo	Definizione	Limite inferiore	Limite superiore	Riferimento
D_{he}	Coefficiente di diffusione dell'elio	0.1	10	[17]
D_{fg}	Coefficiente di diffusione dei gas di fissione	0.1	10	[20]
k_{henry}	Costante di Henry	0.001	1000	[8]
Z_1	Fattore di comprimibilità	0.9	1.5	-
Z_2	Fattore di comprimibilità	0.1	10	-

implica che la scelta dell'equazione di stato (connessa a Z) non sia la priorità nella formulazione della risoluzione termica come ad esempio lo è la costante di Henry.

In conclusione ciò che emerge dall'analisi è che il coefficiente di diffusione e la costante di Henry sono i parametri a cui il modello risulta più sensibile in queste specifiche simulazioni.
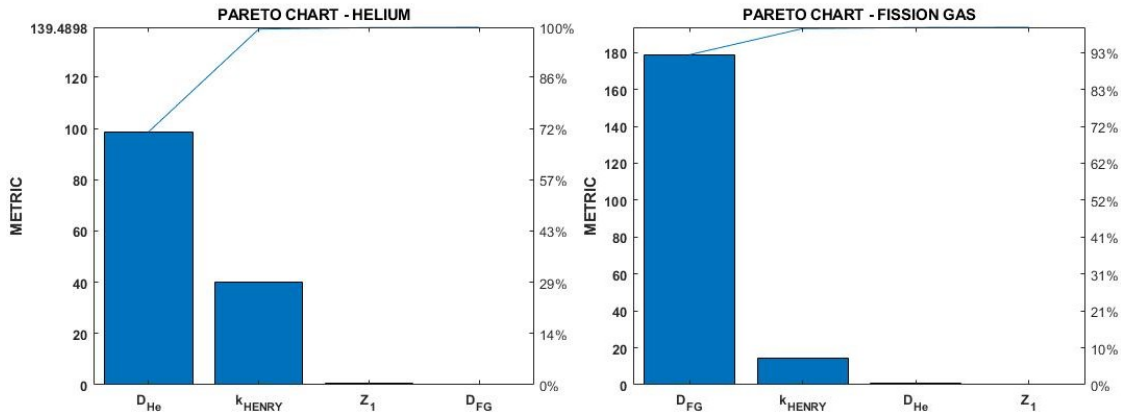
(a) Grafico di Pareto per l'elio a basso burn-up con Z_1.

(b) Grafico di Pareto per i gas di fissione a basso burn-up con Z_1
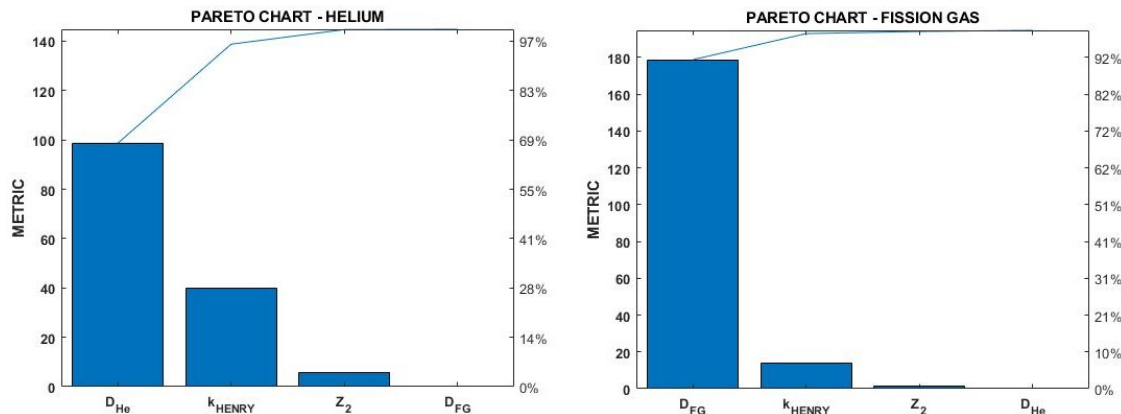
(c) Grafico di Pareto per l'elio a basso burn-up con Z_2.

(d) Grafico di Pareto per i gas di fissione a basso burn-up con Z_2.

Figure 6: Grafici di Pareto a basso burn-up (240 MWd/t$_\text{U}$).

(a) Grafico di Pareto per l'elio ad alto burn-up con Z_1.

(b) Grafico di Pareto per i gas di fissione ad alto burn-up con Z_1.

(c) Grafico di Pareto per l'elio ad alto burn-up con Z_2.

(d) Grafico di Pareto per i gas di fissione ad alto burn-up con Z_2.
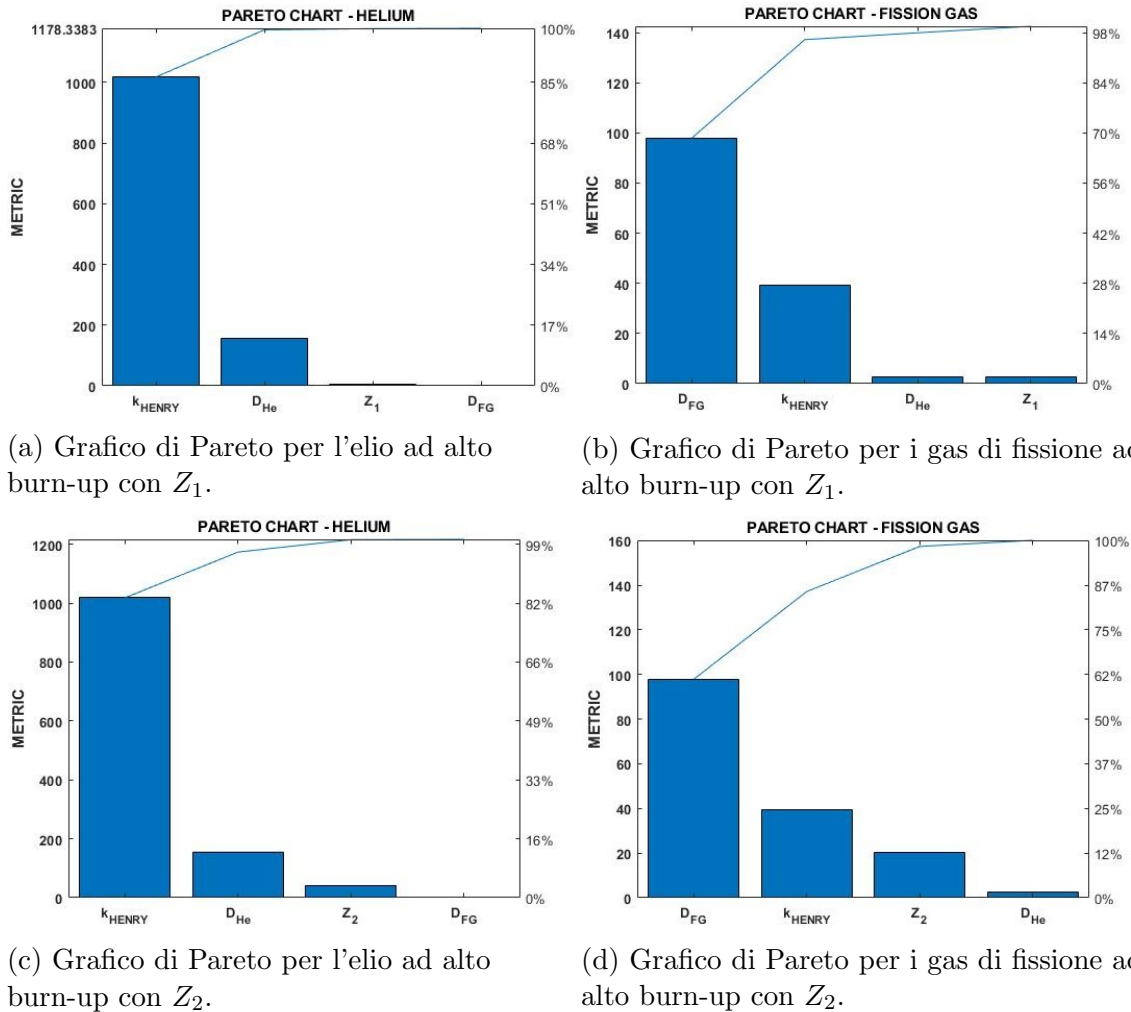
Figure 7: Grafici di Pareto ad alto burn-up (100 GWd/t$_{\mathrm{U}}$).

Conclusione

La tesi propone un modello per descrivere il comportamento intra-granulare dei gas inerti. In questo campo di ricerca costituisce un primo tentativo di accoppiare elio e gas di fissione all'interno del grano di combustibile. Il modello si basa sui processi fisici di diffusione atomica, nucleazione delle bolle, risoluzione ed assorbimento alle bolle. La struttura del sistema lo rende adatto all'applicazione ai codici di *performance* del combustibile nucleare. La prima applicazione del nuovo modello è stata un'analisi esplorativa volta ad identificare le condizioni più interessanti per osservare una possibile interazione tra i gas nel grano. In un'ottica di sinergia tra modellazione ed esperimenti, si propone l'utilizzo di una versione ridotta del modello per accelerare la fase di progettazione e realizzazione di campagne sperimentali in condizioni di *annealing*. Le simulazioni hanno permesso di individuare diversi punti di partenza per la messa a punto di futuri esperimenti sui gas inerti. Il modello predice un'influenza reciproca tra i gas nel grano, soprattutto ad alte concentrazioni

di elio. Per supportare le simulazioni di *annealing* è stata condotta un'analisi di sensitività che attraverso il metodo di Pareto ha individuato i coefficienti di diffusione e la costante di Henry come i parametri la cui incertezza ha un maggiore impatto sul modello. Lo sviluppo futuro del lavoro potrebbe riguardare la validazione del modello all'arrivo di nuovi risultati sperimentali, insieme alla riduzione delle incertezze dei parametri menzionati per migliorare la capacità predittiva del modello. In prospettiva si può pensare di estendere il modello all'analisi di bolle inter-granulari miste. Infine, sarà possibile verificare il modello completo di elio e gas di fissione in esperimenti di irraggiamento di un'intera barretta di combustibile, approfondendo in aggiunta la definizione dei fattori di peso associati alla risoluzione indotta dall'irraggiamento.

Chapter 1

Introduction

The understanding of inert gas behaviour (IGB) in oxide nuclear fuels is essential in optimising fuel usage. Among all the fission products generated in the fuel, the focus of this work is mainly on xenon, krypton and helium. The noble gases xenon and krypton are produced during the fission of uranium and plutonium isotopes in irradiation. Roughly 0.26 stable gas atoms are produced for each fission event [16]. Helium is generated by ternary fissions, (n,α)-reactions on oxygen and α-decays of actinides, which acquire importance in storage conditions [10, 51].

Once produced, the gases can follow two main routes either detrimental to fuel performance. They can be released to the fuel rod free volume causing pressure build-up and thermal conductivity degradation of the rod filling gas. The extent to which the gases are freed from the fuel determines in large part the potential hazard of a reactor core in the event of an accidental cladding breach, which can occur either at the reactor site or during transportation of the spent fuel to a reprocessing plant[25]. On the other hand, inert gases tend to precipitate into bubbles resulting in fuel swelling, which promotes pellet-cladding gap closure and the ensuing pellet-cladding mechanical interaction (PCMI) [23, 28, 43].

In particular, the description of intra-granular gas behaviour is typically the first and fundamental part of models for the prediction of gas release and swelling in nuclear fuel performance codes (FPC). Fuel performance codes have been developed and validated to supply a predictive analysis of the behaviour of nuclear fuel rods under irradiation. The state-of-art modelling of IGB addresses the description of helium and fission gases relying on separate models. This thesis provides a physics-based model that couples their behaviour in the fuel grain and describes the evolution of mixed intra-granular bubbles. It is a first attempt in this field to account for their coexistence in the fuel grain, for this reason experiments on the matter are unavailable. Nevertheless, an experimental program investigating the behaviour of inert gas cocktails in annealing conditions is planned in the frame of different research initiatives. In this regard the model is applied to the simulation of several annealing scenarios with the aim to accelerate the design and the realization of targeted experiments.

The model can be included in fuel performance codes either by direct implementation or via coupling with meso-scale modules. The module adopted in the work is SCIANTIX. It is an open source 0D stand-alone computer code designed to be

included/coupled as a module in existing fuel performance codes [29]. For the purposes of this work, it is used as stand-alone code for the simulation of separate effect experiments at the fuel-grain scale involving inert gas behaviour.

The main steps of the work are the following:

1. Development of a physics-based model describing the coupled intra-granular behaviour of a cocktail of noble gases (helium, xenon and krypton) in UO_2. Formulation of the system of equations and modelling assumptions.

2. Implementation of the model in SCIANTIX. After the verification, the modified code is able to deal with bubbles of pure helium or pure fission gas as well as with mixed intra-granular bubbles.

3. Adoption of a reduced version of the model to simulate its behaviour in annealing conditions. The aim is to find combinations of inert gases in which is likely to observe an interaction between the atom species. The results allow to suggest possible temperature ranges and cocktail compositions that could serve as starting points for the set up of future experiments.

4. As support to the annealing simulations, it is performed a sensitivity analysis using the Pareto method. The goal is to identify those parameters whose uncertainties have the major impact on the model. The outcomes can limit the efforts of future researches to the study of a particular parameter in the attempt to improve the model predictive capability in annealing as well as in irradiation conditions.

The presentation of the work in this text follows in general terms the list above.

Chapter 2 introduces the possible mechanisms influencing the inert gas behaviour in fuel grains and the main parameters adopted for the description of the physical processes. The processes involved are gas atom diffusion, bubble nucleation, resolution from bubbles back into the lattice and gas atom trapping at the bubbles. Each process is described by a suitable model parameter taking into account the differences between helium and fission gas. Particular attention is given to the bubble radius since it represents the variable that links the gases in the mixed bubbles.

Considering the processes described above, Chapter 3 provides the mathematical formulation for the evolution of intra-granular gas bubbles. It results from the combination of two models describing the helium and the fission gas behaviour separately [7, 30]. The seven differential equations that are proposed explain the evolution in time of the gas atom concentrations and the number of bubbles in the grain. In addition two key model parameters are stressed, the irradiation induced and the thermal re-solution. The first one is modelled through a set of three weight factors that allow to consider the homogeneous and the heterogeneous mechanism of re-solution induced by the passage of fission fragments.

The presence of helium requires the assessment of its solubility, related to the thermal re-solution. It is proposed the equation of state that describes the pressure of helium in intra-granular bubbles in order to derive the thermal re-solution term.

The end of the chapter gives an overview of SCIANTIX and outlines the intra-granular structure in the code.

Due to the lack of experimental data concerning cocktails of helium and fission gases, the model developed cannot be validated. To overcome the problem and anticipate future experimental investigations, several annealing scenarios have been simulated in Chapter 4. For these simulations it is sufficient a reduced version of the model. The aim is to find combinations of inert gases in which is likely to observe an interaction between the atom species. The resulting plots lead to a variety of conclusions about the temperature ranges of interest and the regions of dominance of the physical processes involved, i.e. trapping, diffusion and thermal re-solution. These simulations lay the foundation for future experimental investigations on cocktails of inert gases. They enable to identify suitable ranges of gas compositions in the grain, temperature and gas release that could be interesting to explore.

Finally, in Chapter 5 a sensitivity analysis is performed with the Pareto method in order to identify the parameters whose uncertainty has the major impact on the model results. The selected parameters describe the main processes governing the gas behaviour during the annealing simulations, i.e. the diffusion coefficient, Henry's constant and the compressibility factor. The outcomes of the analysis can support the results of the annealing tests and limit the efforts to the improvement of a particular parameter.

The production and the behaviour of gaseous fission products (i.e., xenon, krypton, and helium) in the fuel matrix, both in irradiation and storage, affect the fuel microstructure. Their presence in the fuel can ultimately lead to two complementary phenomena, swelling and fission gas release. This thesis combines the models for the inert fission gases and helium in irradiated fuels that are integrated in SCIANTIX and can be applied to fuel performance codes. The model in fact is kept as simple as possible in view of the efficient application to integral fuel rod analysis, the related stringent computational cost requirements and the uncertainties associated to some of the model parameters. Three specific topics are addressed: (1) the description of the parameters and the processes involved in the intra-granular behaviour of inert gases; (2) the model equations governing the IGB are detailed together with specific parameters (i.e., irradiation induced re-solution, equation of state for helium and thermal re-solution); (3) simulations to test the model behaviour in annealing conditions together with a sensitivity analysis on a few model parameters.

The conclusions and the perspectives of this thesis are presented in the final chapter.

Chapter 2

Intra-granular processes

Abstract

The present chapter aims at describing the fundamental processes that control the formation and evolution of intra-granular bubbles in nuclear fuel. The processes involved are gas atom diffusion, bubble nucleation, re-solution from bubbles back into the lattice with distinction between irradiation induced and thermal re-solution and lastly, gas atom trapping at the bubbles. A description of each of these phenomena will be introduced through the use of model parameters, in the framework of rate theory modelling. The proposed parameters are a direct consequence of the hypotheses assumed for the development of the model. It is outlined the peculiarity of helium behaviour in oxide fuels compared to fission gases that comes from its higher solubility and diffusivity. The radius of intra-granular bubbles is addressed separately due to its role in the model. It represents the connection among the atoms in the bubbles.

2.1 Diffusion

The first and basic step after gas production is single gas atom diffusion in the lattice. Intra-granular gas diffusion to grain boundaries provides the source term for the inter-granular processes[1], ultimately leading to grain-boundary gaseous swelling and fission gas release [26, 46, 50]. Compared to xenon and krypton, helium presents a higher diffusivity in oxide nuclear fuel [2]. It is in fact a critical property for helium. Due to this behaviour, the diffusion coefficients describing the diffusivity vary according to the type of atom.

- Helium Diffusion

  Luzzi et al.[17] proposed a helium diffusion coefficient D (m^2 s^{-1}) recommended for infused samples with zero or very limited lattice damage and valid in the temperature range 968-2110 K, i.e.:

$$D_{He} = 2 \times 10^{-10} \exp\left(\frac{-2.12 \text{ eV}}{k_B T}\right) \tag{2.1}$$

  where k_B (J K^{-1}) is Boltzmann's constant, T (K) temperature.

---

[1] Inter-granular processes are not part of this thesis.

- Fission Gas Diffusion

  Diffusion has large potential for FGR (Fission Gas Release) fractions. The diffusivity of FG (Fission Gas) in oxide nuclear fuels is a function of temperature, stoichiometry and fission rate. Turnbull et al.[40] published the following expression for the diffusion coefficient D:

$$
\begin{aligned}
D &= D_1 + D_2 + D_3 \\
D_1 &= 7.6 \times 10^{-10} \exp\left(-4.86 \times 10^{-19}/k_B T\right) \\
D_2 &= 5.64 \times 10^{-25} \sqrt{\dot{F}} \exp\left(-1.91 \times 10^{-19}/k_B T\right) \\
D_3 &= 2.0 \times 10^{-40} \dot{F}
\end{aligned}
\tag{2.2}
$$

  where the single gas atom diffusion coefficient D is expressed in $m^2\ s^{-1}$. D_1 denotes the intrinsic diffusion which depends only on the fuel temperature (T) and is dominant above 1400°C, D_2 describes diffusion via thermal and irradiation induced cation vacancies, it depends both on the fuel temperature and the fission rate density ($\dot{F}$) and dominates when 1000°C < T < 1400°C, D_3 corresponds to the athermal term and dominates down to 250°C [44].

- Bubble diffusion

  Different forces may affect bubble motion, such as the thermal gradient, the stress gradient, moving dislocations and shifting grain boundaries [44]. The intra-granular model currently assumes that larger clusters (bubbles) are immobile, leaving out a detailed analysis of these phenomena and including the diffusion term only for single gas atoms. This assumption is supported by the work of Verma et al.[47]. The work reports that the intra-granular bubble migration in the grain cannot account for the large FGR which is observed during post-irradiation annealing experiments. This mechanism is still under investigation.

2.2   Nucleation

Nucleation process refers to the formation of bubbles. According to the terminology of Olander and Wongsawaeng [27], there are two different nucleation mechanisms acting and competing in fuel grains, i.e. heterogeneous and homogeneous mechanism. Each of these processes is modelled introducing a specific rate of nucleation occurrence.

- Heterogeneous nucleation

  Heterogeneous nucleation refers to the nuclei of the new bubbles being created as a direct consequence of the interaction of fission fragments with the lattice. Vacancy clusters formation in the wake of fission fragments provide the nuclei of the new bubbles. The rate of bubble nucleation per unit volume is:

$$
\nu_{het} = 2\dot{F}\alpha
\tag{2.3}
$$

where ν_{het} (nucleated bubbles m^{-3} s^{-1}) is the nucleation rate, the factor 2 accounts for the number of fission fragments per fission, $\dot{F}$ is the fission rate density (fissions m^{-3} s^{-1}) and α (nucleated bubbles per fission fragment) is a number that in literature ranges from 5 to 25 [1, 39].

- Homogeneous nucleation

  Homogeneous mechanism refers to bubbles being nucleated by diffusion-driven interactions of dissolved gas atoms [35, 48]. The rate of production of dimers (diatomic gas clusters), which are the first product of homogeneous nucleation, is:

$$\nu_{hom} = f_N k_N c^2 \tag{2.4}$$

  where ν_{hom} corresponds to nucleated dimers m^{-3} s^{-1} , c is the concentration of atoms in the solid (at m^{-3}), k_N is the rate constant depending on diffusivity and radius of atoms and f_N is called the nucleation factor. For a clearer exposition of these terms refer to [27]. Equations should be written for trimers, tetramers, etc. but this would increase the complexity of the mathematical problem. In a strong simplification, it is assumed that upon creation of dimers bubbles contain a unique but time dependent average number of gas atoms n.

For the purpose of this work it is assumed that the heterogeneous nucleation mechanism is dominant in oxide fuels, so SCIANTIX code only adopts equation 2.3. Furthermore, it is considered only a single bubble size and a single bubble density. The "single-size" model will be discussed and motivated in Section 3.1.

2.3 Re-solution

There is a continuous flow of gas atoms between the bubbles and the solution, so the re-solution term must be included. It can be divided in irradiation induced re-solution and thermal re-solution according to the driving mechanism. For the fission gases, re-solution is (primarily) irradiation-driven [16, 18]. The same way of nucleation, irradiation induced re-solution is classified adopting the terminology of Olander and Wongsawaeng [27], i.e. heterogeneous and homogeneous. Solubility is not usually considered for xenon and krypton as discussed by Lösönen [16], for this reason thermal re-solution is only referred to helium.

2.3.1 Irradiation induced re-solution

Although γ-rays, neutrons and fission fragments are all capable of causing re-solution of fission gases from bubbles, it is only the fission fragment that can account for the high efficiency of the process as observed experimentally. Fission fragments not only have a higher initial kinetic energy (50-100 MeV) than fast neutrons (2 MeV), but they are also charged and consequently have a higher cross-section for transferring energy either to lattice, or to gas atoms [44].

- Heterogeneous re-solution

  Heterogeneous re-solution refers to bubbles being destructed en-bloc by passing fission fragments. The re-solution parameter proposed by Turnbull [39] is

  $$b_{het} = \frac{re - solved\ bubbles}{bubble\ unit - time} = 2\pi\mu_{ff}(R_{ff} + R)^2\dot{F} \tag{2.5}$$

  where b_{het} is the re-solution rate (s^{-1}), μ_{ff} (m) and R_{ff} (m) are the average length and radius of a fission spike, respectively, and R (m) is the radius of the gas bubble. The factor 2 reflects the two fission fragments per fission and $\dot{F}$ is the fission rate density (fissions m^{-3} s^{-1}).

- Homogeneous re-solution

  Homogeneous mechanism occurs gradually by ejection of individual atoms by collisions with fission fragments. The re-solution parameter can be expressed by

  $$b_{hom} = \frac{re - solved\ atoms}{atom\ unit - time} \tag{2.6}$$

  The reciprocal of this term is the mean time that an atom spends in a bubble [27].

In contrast to nucleation, the model proposed in Section 3.1 adopts homogeneous and heterogeneous mechanisms for the irradiation induced re-solution.

2.3.2 Thermal re-solution

One of the main reasons of the peculiarity of helium behaviour in oxide fuels compared to fission gases comes from its higher solubility [21, 22, 36]. The solubility demands a model that includes thermal re-solution. In the presentation of this parameter the work of Cognini et al.[7] has been followed. It has been verified that helium solubility in oxide nuclear fuel is linearly proportional to the infusion pressure at a fixed temperature [21, 22, 33, 36]. This double dependence leads to the expression

$$C_{S,He}(\text{at m}^{-3}) = k_H p \tag{2.7}$$

where k_H (at m^{-3} MPa^{-1}) is Henry's constant and p (MPa) is the helium pressure. It is recalled that the subject of this study is a cocktail of helium and FG, therefore, helium exercises a partial pressure in the spherical bubbles. The evaluation of pressure in intra-granular bubbles is postponed to Chapter 3.

Assuming that Henry's law is valid for the He-UO$_2$ system [2], Henry's constant is a temperature function [8, 32]. Figure 2.1 shows the experimental values of Henry's constant in UO$_2$, the categorization is based on the sample microstructure, i.e., powders and single crystals [8].

---

[2]The validity of Henry's law in the system is verified with a small dataset by Sung [36]. At each of three temperatures (1473 K, 1623 K, 1773 K) he performed infusions at three pressures (4.8 MPa, 6.9 MPa, 9.0 MPa) in a UO$_2$ single crystal. The resulting solubilities show a linear dependency on pressure at each temperature, corroborating the verification of Henry's law.

It is reported the best estimate correlation[3] obtained by Cognini et al.[8] for single crystals and valid in the temperature range of 1073-1773 K :

$$k_H = 4.1 \times 10^{24} \exp\left(\frac{-0.65 \text{ eV}}{k_B T}\right) \tag{2.8}$$

where k_B (J K^{-1}) is Boltzmann's constant and T (K) the temperature. The last correlation is suitable for calculations in mesoscale models dealing with single fuel grains and it is adopted in the current model.

In conclusion thermal re-solution is represented by the term $\beta k_H p$ where β is the trapping rate by Ham [14]:

$$\beta = 4\pi D_{He} R_{ig} N_{ig} \tag{2.9}$$

where R_{ig} (m) is the radius of intra-granular bubbles, N_{ig} (bubbles m^{-3}) is the intra-granular bubble density and D_{He} is helium diffusivity (m^2 s^{-1}).
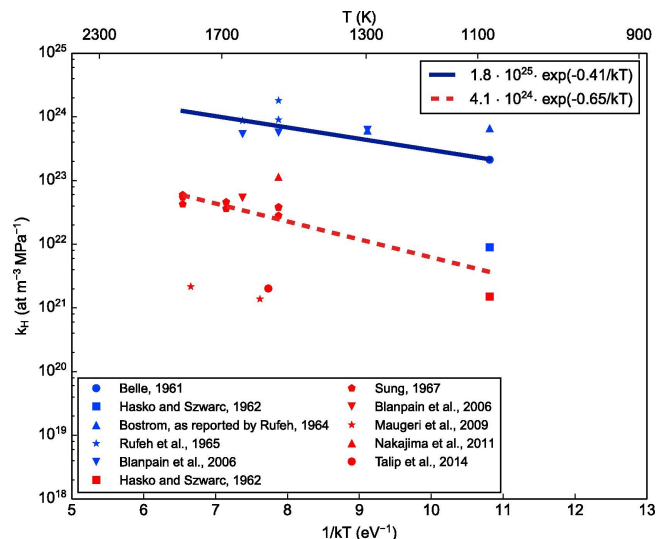
Figure 2.1: Plot of the experimental Henry's constant of helium classified depending on the microstructure of the sample (i.e. blue for the powder samples and red for the single crystal samples). Each cluster is fitted by a distinct correlation (bordeaux and blue navy).

2.4 Trapping

Gas atom migration in nuclear fuels involves more than simple lattice diffusion. Bubbles increase in size principally by trapping during diffusion of single gas atoms. The formulation derived by Ham [14] is adopted

$$g = \frac{trapped \ atoms}{atom \ unit - time} = 4\pi D(R_{ig} + R_{at})N_{ig} \tag{2.10}$$

where g is the trapping rate (s^{-1}), R_{ig} (m) is the radius of intra-granular bubbles, R_{at} is the atomic radius (m), N_{ig} (bubbles m^{-3}) is the intra-granular bubble density

---

[3]Sometimes it is seen the inverse function of k_H.

and D (m^2 s^{-1}) is the single-atom diffusion coefficient.

Figure 2.2 summarizes the possible mechanisms that involve helium and fission gas in the fuel grain.
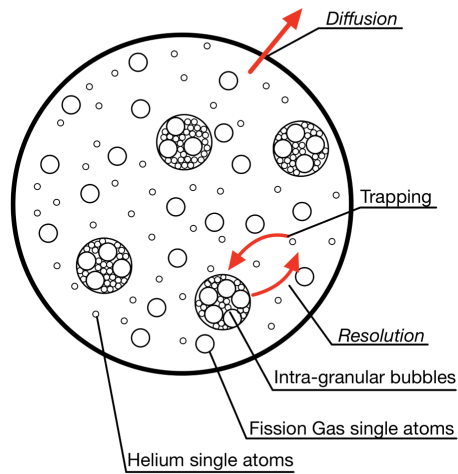
Figure 2.2: Sketch representing the mechanisms involved in the fuel grain.

2.5 Bubble radius

Bubble radius is another important parameter in the description of intra-granular gas behaviour, mainly because it considers the coexistence of helium and FG. Furthermore, it is useful to evaluate the thermal re-solution of helium atoms in lattice. Following the assumptions of Clement and Wood [6] and Fell and Murphy [13], clusters are made of only gas atoms and vacancy absorption at the clusters is neglected. An additional and relevant assumption is that bubbles are spherical. As a consequence, the volume of the bubbles (m^3) containing n gas atoms is calculated with the formula:

$$V_{ig} = n_{He}V_{He} + n_{FG}V_{FG} = \frac{4}{3}\pi R_{ig}^3 \tag{2.11}$$

The radius of intra-granular bubbles (m) is obtained from the inverse of equation 2.11:

$$R_{ig} = \left[\frac{3}{4\pi}(n_{He}V_{He} + n_{FG}V_{FG})\right]^{1/3} \tag{2.12}$$

where n (at bubble^{-1}) is different between helium and FG. V_{He} is the atomic volume of helium and corresponds to 7.8×10^{-30} m^3 [7]. For FG the atomic volume in bubble is 4.09×10^{-29} m^3 equal to the volume of the Schottky defect [15]. Choosing the atomic volume as equal to the volume of the Schottky defect is consistent with the assumption that the gas atoms in the bubbles completely occupy available vacancies [30].

Chapter 3

Physical model

Abstract

The model proposed in this chapter describes the coupled intra-granular behaviour of a cocktail of noble gases composed by helium, xenon and krypton. It is presented the system of equations regulating the evolution of intra-granular bubbles. The novelty of this model lies in the fact that it is a first attempt to combine helium and fission gas in intra-granular bubbles. Therefore the necessity to include both the irradiation induced and the thermal re-solution, the latter in fact characterizes helium solubility. To provide a more detailed representation of the inert gas behaviour, the homogeneous and the heterogeneous mechanisms of irradiation induced re-solution are included in the model through a set of three weight factors. Even if the irradiation induced re-solution will not be considered in the simulations of the next chapter, it is now mentioned as basis for the future development of the model in irradiation conditions. The importance of helium solubility requires a further examination. The first step for evaluating the solubility is the assessment of the helium pressure within intra-granular bubbles, performed with the use of an equation of state. It is then derived the final formulation for the thermal re-solution which is dependent on the choice of the helium pressure. The model has been implemented in SCIANTIX. To conclude the chapter it is given a brief description of the mentioned code. As a result of the work done, SCIANTIX is able to deal with pure helium or fission gas bubbles as well as with mixed bubbles.

3.1   Mathematical model

The model presented in this section describes the coupled intra-granular behaviour of a cocktail of noble gases (helium, xenon and krypton) in UO_2. It results from the evolution of intra-granular bubble population through the physical processes introduced in chapter 2.

It is a physics-based model, this choice allows the application to different materials by adapting the fundamental parameters.

In its final form the model consists of seven differential equations, three of them are referred to FG behaviour, three to helium behaviour and the last one refers to the number of bubbles containing both the atom species.

The equations proposed for helium derive from the work of Speight [34] and Cognini et al. [7]. The latter in fact has a fission-gas-inspired model structure, that brings about the possibility to explicitly account for the interaction between helium and fission gas [7]. On the other side the fission gas formulation refers to the single-size model of Pizzocri et al. [30].

The system has time dependent solutions, a space-discretization based solution would require a high computational effort, impractical for the application in fuel performance codes.

The following equations have been directly implemented in SCIANTIX (Section 3.5).

Fission gas

$$\frac{\partial c_{FG}}{\partial t} = S_{FG} + D_{FG}\nabla^2 c_{FG} - g_{FG}c_{FG} + b_{FG}m_{FG} - \nu n_{FG} \tag{3.1}$$

$$\frac{\partial m_{FG}}{\partial t} = g_{FG}c_{FG} - b_{FG}m_{FG} + \nu n_{FG} \tag{3.2}$$

$$\frac{\partial n_{FG}}{\partial t} = g'_{FG}c_{FG} - b'_{FG}n_{FG} \tag{3.3}$$

Helium

$$\frac{\partial c_{He}}{\partial t} = S_{He} + D_{He}\nabla^2 c_{He} - g_{He}c_{He} + b_{He}m_{He} + \gamma m_{He} - \nu n_{He} \tag{3.4}$$

$$\frac{\partial m_{He}}{\partial t} = g_{He}c_{He} - b_{He}m_{He} - \gamma m_{He} + \nu n_{He} \tag{3.5}$$

$$\frac{\partial n_{He}}{\partial t} = g'_{He}c_{He} - b'_{He}n_{He} - \gamma n_{He} \tag{3.6}$$

Number of bubbles

$$\frac{\partial N}{\partial t} = \nu - b''N \tag{3.7}$$

where the main variables are c the gas grain solution concentration (at m^{-3}), m the gas grain bubbles concentration (at m^{-3}), n atoms per intra-granular bubbles (at bubble^{-1}) and N the density of bubbles (bubbles m^{-3}). The subscripts identify fission gas (FG) and helium (He).

S is the atoms source rate [4] (at m^{-3} s^{-1}), γ is the thermal re-solution rate (s^{-1}) examined in 3.4. The diffusion coefficient D, the trapping rate g, the irradiation induced re-solution b and the nucleation rate ν are discussed in detail in chapter 2. Considering the bubbles, g' corresponds to $\frac{g}{N}$ and it is the trapping rate of bubbles (m^3 bubble^{-1} s^{-1}). b' and b'' represent the homogeneous and the heterogeneous re-solution rate (s^{-1}) respectively.

---

[4]S_{FG} depends on the product of the fission yield y and the fission rate $\dot{F}$. S_{He} includes ternary fissions, (n,α)-reactions on oxygen and α-decays [4, 11, 12].

Some assumptions about the parameters are briefly recalled in the following.

The diffusivity is different for helium and fission gas, while bubbles don't diffuse in the grain. Since bubbles are immobile, bubble coalescence (merger of two or more bubbles) is neglected. Only heterogeneous nucleation is taken into account, because major experimental and theoretical works agree on the dominance of the heterogeneous mechanism over the homogeneous one [1, 19, 39]. The irradiation induced re-solution is homogeneous and heterogeneous. Thermal re-solution is exclusively considered for helium.

Equations $(3.1)-(3.7)$ are closely inter-related to each other through the relation among m, N and n, the re-solution and nucleation parameters.

The intra-granular bubble population is described by a single bubble size and a single bubble number density, this approach is called single-size model. Bubbles nucleates instantaneously at the average size and are destructed according to the heterogeneous mechanism always at the average size. The single-size model is motivated by TEM observations showing that the bubble radii are confined to a narrow range [27]. In general bubbles are created/destructed at different sizes. In order to calculate the average number of atoms in a bubble (n), the effects of nucleation and re-solution are included through the equations for m and N. The same way of Pizzocri et al.[30], the model starts from a cluster dynamics approach to introduce these bubble-distribution related effects, but ends with a formulation that only includes average values for n.

Initial conditions

The model requires the initial conditions for m, c, n, N and the grain radius a. They can be introduced as external inputs in the SCIANTIX code. An example of initial conditions is reported in Section 4.1.

Boundary conditions

The boundary conditions (BC) assumed for the single-atoms diffusion problem are the same for helium and fission gas:

$$c(a) = 0 \tag{3.8}$$

$$\left(\frac{\partial c}{\partial r}\right)_{r=0} = 0 \tag{3.9}$$

where a is the grain radius (m) and c is the gas grain solution concentration (at m^{-3}). The first BC implies that when atoms reach the grain boundary, they find a perfect sink and can't re-enter the grain. This condition brings along two additional assumptions that simplify the model and the study of the phenomena in the grain. The first assumption considers the grain as spherical [3].

The second one implies that the inter-granular pressure p_{gb} at the grain boundaries is null. Helium solubility at grain boundary is dependent on p_{gb} according to the formula $c_{He}(a) = k_H p_{gb}$ [7]. Equation 3.8 becomes acceptable for helium if the application of the model is limited to experiments performed in vacuum, where $p_{gb} \approx 0$.

This is a simplified version of the model but since the focus of the work is on the intra-granular bubbles, grain boundary phenomena can be considered less relevant. Equation 3.9 implies the symmetry for the concentration of the gas in the grain domain.

3.2 Mechanisms of irradiation induced re-solution

The model considers two ways through which gas atoms can leave the bubbles. Using the parameters b' and b'' both the homogeneous and the heterogeneous mechanisms can be included in the irradiation induced re-solution, allowing a more detailed representation of inert gas behaviour. Even if the irradiation induced re-solution will not be considered in the simulations of Chapter 4, it is now mentioned as basis for the future development of the model in irradiation conditions. The total irradiation induced re-solution rates for helium and fission gas are

$$b_{He} = b'_{He} + b'' \tag{3.10}$$
$$b_{FG} = b'_{FG} + b'' \tag{3.11}$$

where b' is the atoms in bubbles re-solution rate (s^{-1}), b'' is the bubbles re-solution rate (s^{-1}). b'' coincides for helium and fission gas, because it refers to the heterogeneous mechanism according to which the bubble is completely destroyed by a passing fission fragment. b' depends on the type of atom and refers to the homogeneous re-solution. When bubble destruction happens, it affects helium and FG populations independently from the atom species, while the knock-out of one gas atom at a time influences the specific atom population.

The rates of these mechanisms are not the same since they consider different parameters [5]. In the case of fission gas, the ratio of the homogeneous re-solution rate to the heterogeneous rate is $\sim 10^{-3}$ [27, 24].

In order to account for these different contributions, a set of three weight factors (w_{He}, w_{FG}, w_N) is introduced. Weight factors allow the conservation of the re-solution parameter b in the model:

$$b = b'_{He} + b'_{FG} + b'' \tag{3.12}$$

where

$$b'_{He} = w_{He}b$$
$$b'_{FG} = w_{FG}b \tag{3.13}$$
$$b'' = w_N b$$

It can be observed that it is required just one formula for all these re-solution rates, i.e. the formula for b. SCIANTIX adopts the mathematical expression of the heterogeneous re-solution [39]. The expression for the homogeneous re-solution b' can be neglected, because the parameter is simply obtained scaling b.

Equations 3.12 and 3.13 lead to a formulation that links proportionally the weight factors:

$$1 = w_{He} + w_{FG} + w_N \tag{3.14}$$

One factor can be obtained from the others by uniformly scaling (enlarging or reducing). Fixed w_{He} and w_{FG}, the value of w_N is obtained from equation 3.14 to maintain the proportionality. Furthermore, this scaling allows to keep the proportionality among m, n and N, remembering that $m = nN$. The extreme cases, in which w_{He} or w_{FG} are equal to one, correspond to pure helium bubbles or pure

---

[5]Refer to section 2.3 for the mathematical formulations.

fission gas bubbles, respectively. It is important to note that the values of w_{He} and w_{FG} used in the code are arbitrary constants, there are no references in the literature about these factors. A more in-depth study is necessary to assess their values, but at the first stages of development of this model the choice of arbitrary constants is acceptable.

The consequences of the use of weight factors are not limited to the model but also to the role of re-solution in the fuel grain. Irradiation induced re-solution of the gas from bubbles is meaningful, because it significantly increases the gas population in the fuel matrix which is capable of diffusing out of the grains. Via the release, inert gases have an impact on the inner pressure of the rod and the fuel-cladding gap conductivity.

For the sake of completeness the balance equations for m, n and N with respect to the irradiation induced re-solution rate are reported below.

$$\frac{d(m_{He} + m_{FG})}{dt} = \frac{d\left(N(n_{He} + n_{FG})\right)}{dt} = N\frac{dn_{He}}{dt} + N\frac{dn_{FG}}{dt} + (n_{He} + n_{FG})\frac{dN}{dt} \quad (3.15)$$

The different terms of the equation are analyzed separately and it is considered the re-solution parameter only:

$$N\frac{dn_{He}}{dt} = N\left(-b'_{He}n_{He}\right)$$
$$N\frac{dn_{FG}}{dt} = N\left(-b'_{FG}n_{FG}\right) \quad (3.16)$$
$$(n_{He} + n_{FG})\frac{dN}{dt} = (n_{He} + n_{FG})\left(-b''N\right)$$

Combining equations 3.15 and 3.16 the balance is verified as follows:

$$\frac{d(m_{He} + m_{FG})}{dt} = -(b'_{He} + b'')m_{He} - (b'_{FG} + b'')m_{FG} = -b_{He}m_{He} - b_{FG}m_{FG} \quad (3.17)$$

3.3 Equation of state

The solubility term calls for the necessity of evaluating the helium pressure within intra-granular bubbles as anticipated in Section 2.3[6].

This work follows the procedure of Cognini et al. [7] with regards to the choice of the equation of state (EOS) for the bubbles and the derivation of the thermal re-solution (Section 3.4).

Clearly, the coexistence of helium and FG inside the bubbles requires a different view of the problem. In fact the first assumption comes from the consideration that, since bubbles are composed by different atom species, each one exercises its own pressure inside the bubble. As consequence the total pressure of the bubble results from a combination of these contributions.

According to Dalton's law of partial pressures, the total pressure exercised by a mixture of gases is equal to the sum of the partial pressures of each of the constituent gases, in this case:

$$p_{ig} = p_{FG} + p_{He} \qquad (3.18)$$

where p_{ig} (Pa) is the total pressure within intra-granular bubbles.

Dalton's law can also be expressed using the mole fraction of a gas (x). The mole fraction of helium is expressed as

$$x_{He} = \frac{n_{He}}{n_{He} + n_{FG}} \qquad (3.19)$$

where n corresponds to atoms per bubble. The partial pressure of helium is

$$p_{He} = x_{He} p_{ig} = \frac{n_{He}}{n_{He} + n_{FG}} p_{ig} \qquad (3.20)$$

To link the bubble pressure to the temperature and the volume of the gases the EOS of Carnahan–Starling [5] is applied

$$p_{ig} = \frac{k_B T Z}{V_{at}} \qquad (3.21)$$

where k_B (J K^{-1}) is the Boltzmann's constant, T (K) the temperature, V_{at} is the volume of the gas atom (m^3) and Z the compressibility factor.

It is known that Dalton's law is formulated for ideal gases and ignores interactions of unlike atoms. The deviation from the ideal behaviour is taken into account through the introduction of the compressibility factor Z in the formula of the bubble pressure p_{ig}. The choice of the EOS is consistent with other literature data [7, 42], but remains difficult to validate. However, as shown in Chapter 4, the compressibility Z and as consequence the pressure are not crucial parameters compared to Henry's constant or the diffusion parameter, whose uncertainties are more relevant in determining the gas behaviour in fuel grains.

In order to give a complete description of the problem it is reported the formula for compressibility factor:

$$Z = \frac{(1 + y + y^2 - y^3)}{(1 - y)^3} \qquad (3.22)$$

---

[6]The pressure of fission gases is not evaluated, because their solubility is neglected as mentioned in the same section.

with y the volumetric fraction of gas and d the diameter of hard sphere (m) given respectively by

$$y = \frac{\pi d^3}{6 V_{at}} \tag{3.23}$$

and

$$d \text{ (m)} = 2.973 \ 10^{-10} \left[0.8414 - 0.05 \ln \left(\frac{T}{10.985} \right) \right] \tag{3.24}$$

The hard sphere diameter has been determined by Van Brutzel [42], whose study takes into account the interactions between the helium atoms inside nanobubbles and the surrounding UO$_2$ matrix.

In order to identify a suitable pressure for the bubbles, it is adopted an average atomic volume (m^3) expressed as follows

$$V_{at} = \frac{V_{ig}}{n_{tot}} \tag{3.25}$$

where V_{ig} is the bubble volume (m^3) and n_{tot} is the total number of atoms (helium, xenon and krypton) per bubble. The resulting atomic volume will be different from the real atomic volumes of helium and fission gases. However it seems reasonable to consider as first approximation that this term hasn't a big impact on the model compared to other parameters.

Eventually, combining equation 3.20 and 3.21, helium pressure introduced in the model corresponds to

$$p_{He} = \left(\frac{k_B T Z}{V_{ig}} n_{tot} \right) x_{He} = \frac{k_B T Z}{V_{ig}} n_{He} \tag{3.26}$$

3.4   Formulation of the thermal re-solution

It is now presented the final formulation for the thermal re-solution of helium in intra-granular bubbles. Thermal re-solution contains both the equation of state of intra-granular bubbles and Henry's constant, which is poorly characterised experimentally. It is recalled that helium solubility is equal to

$$C_{S,he} = k_H p_{He} \tag{3.27}$$

where k_H (at m^{-3} MPa^{-1}) is Henry's constant and p_{He} (MPa) is the helium partial pressure obtained in the previous section. To account for the thermal re-solution in the model, the trapping rate β (s^{-1}) is introduced and multiplied for the helium solubility, i.e. $\beta k_H p_{He}$.
Considering the trapping rate by Ham [14]

$$\beta = 4\pi D_{He} R_{ig} N_{ig} \tag{3.28}$$

and combining equations 3.26 and 3.28, it can be written:

$$\beta k_H p_{He} = \left(4\pi D_{He} R_{ig} k_H \frac{k_B T Z}{V_{ig}}\right)(n_{He} N_{ig}) = \gamma m_{He} \tag{3.29}$$

where D_{He} is the helium diffusion coefficient (m^2 s^{-1}), R_{ig} is the bubble radius (m), k_H is Henry's constant (at m^{-3} MPa^{-1}), k_B is the Boltzmann's constant (J K^{-1}), T is the temperature (K), Z is the compressibility factor and V_{ig} is the bubble volume (m^3). The multiplication of the variables n_{He} and N_{ig} gives the number of helium atoms inside the bubbles m_{He} (at m^{-3}). The resulting formula for the thermal re-solution rate (s^{-1}) is:

$$\gamma = 4\pi R_{ig} D_{He} k_H \frac{k_B T Z}{V_{ig}} \tag{3.30}$$

The thermal re-solution is dependent on the choice of the EOS for the bubbles. Different equation of states will imply different formulas for γ [16].

3.5   SCIANTIX computer code

Nuclear fuel performance modelling is one of the fundamental activities required for the safety analysis, design optimization and operation of nuclear reactors. Modelling is performed using dedicated computer codes. They have been developed following two main categories based on the conditions of operation to be simulated, normal or accidental conditions [45]. Modelling of fission gas behaviour is a crucial aspect in fuel performance codes, since they have an impact on the operation of nuclear fuel. The concentrations of gaseous fission product elements (principally Xe, Kr and He) are required for fission gas swelling and release models.

The SCIANTIX code presented in the paper of Pizzocri et al.[29, 37] aims at bridging lower-length scale and engineering scale of fuel performance codes. SCIANTIX has been designed to be included/coupled as a module in existing fuel performance codes or can be used as a stand-alone code. In this work it has been used as a stand-alone code for the simulation of the inert gas behaviour at the fuel-grain scale.

Part of this thesis work has been spent for the implementation in SCIANTIX of the model previously described. As a result of the work done, the different gas models in SCIANTIX can remain decoupled or they can interact leading to mixed gas bubbles. It is proved in Appendix B that the new coupled path does not interfere with the separated paths.

The flow chart reported in 3.1 shows a general structure of the code. On the left it is reported the external driver (referred to as parent code) and on the right the SCIANTIX module itself. The parent code performs several fundamental operations, e.g., input reading, output printing, and time stepping. In the stand-alone mode the inputs for the parent code are decided from the user. At each time step, the SCIANTIX module performs the incremental calculation of the evolution of physical state variables, in this case the figures of merit are the inert gas concentrations. Referring to the intra-granular behaviour, from the external input parameters it is possible to choose separated models for helium and fission gas or the coupled model. The scheme followed by SCIANTIX is proposed in Figure 3.2. The block of diffusion solves the three equations for c, m and n, separately for helium and fission gas (Eq. 3.1-3.6). The block of the mixed intra-granular behaviour performs the calculation of N (Eq. 3.7) and the bubble radius R_{ig} in the case of mixed bubbles.

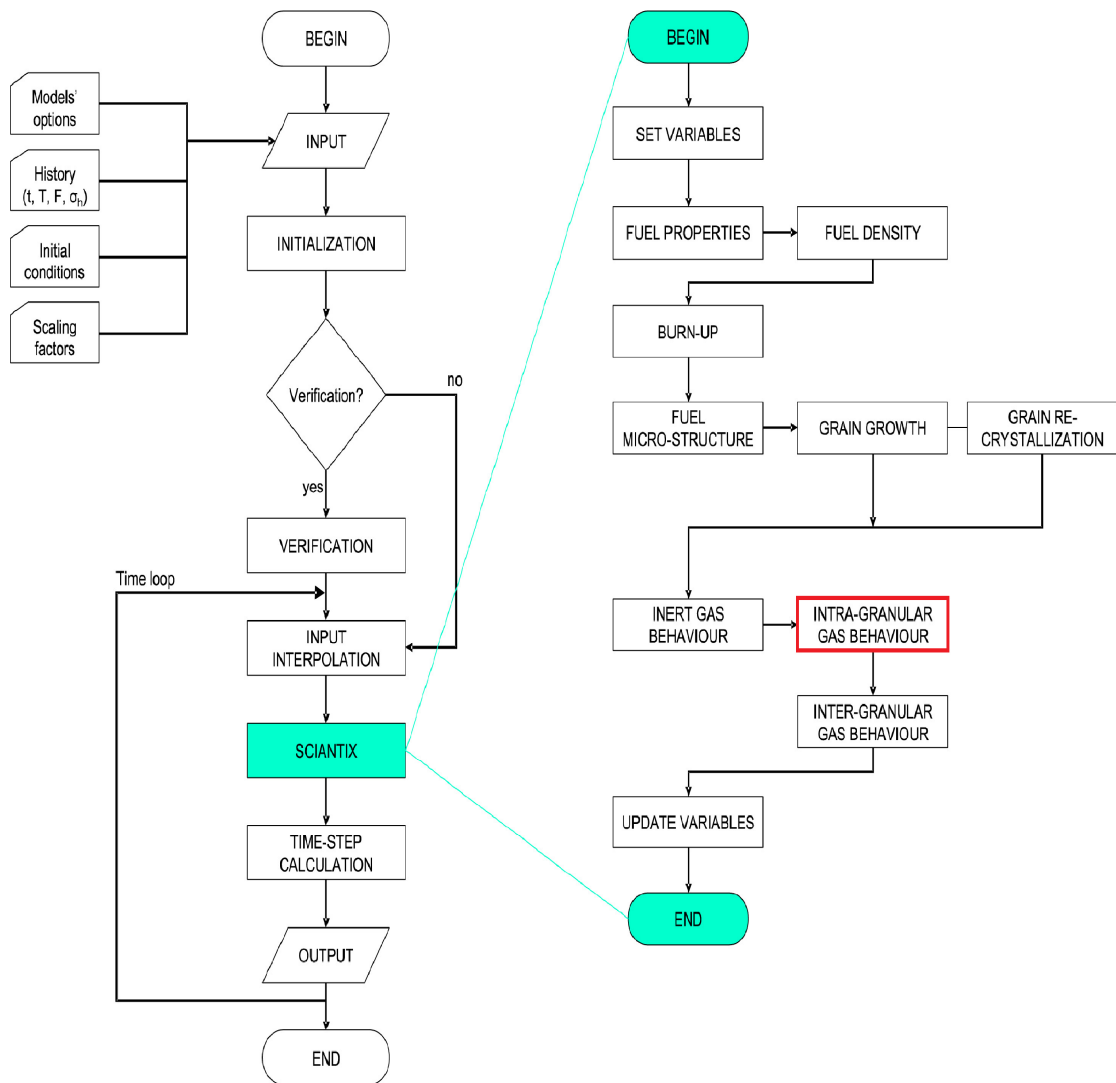The simulations described in Chapter 4 are obtained from SCIANTIX.

Figure 3.1: Flow chart of SCIANTIX, highlighting the division between the external driver (parent code) and the meso-scale module [29].
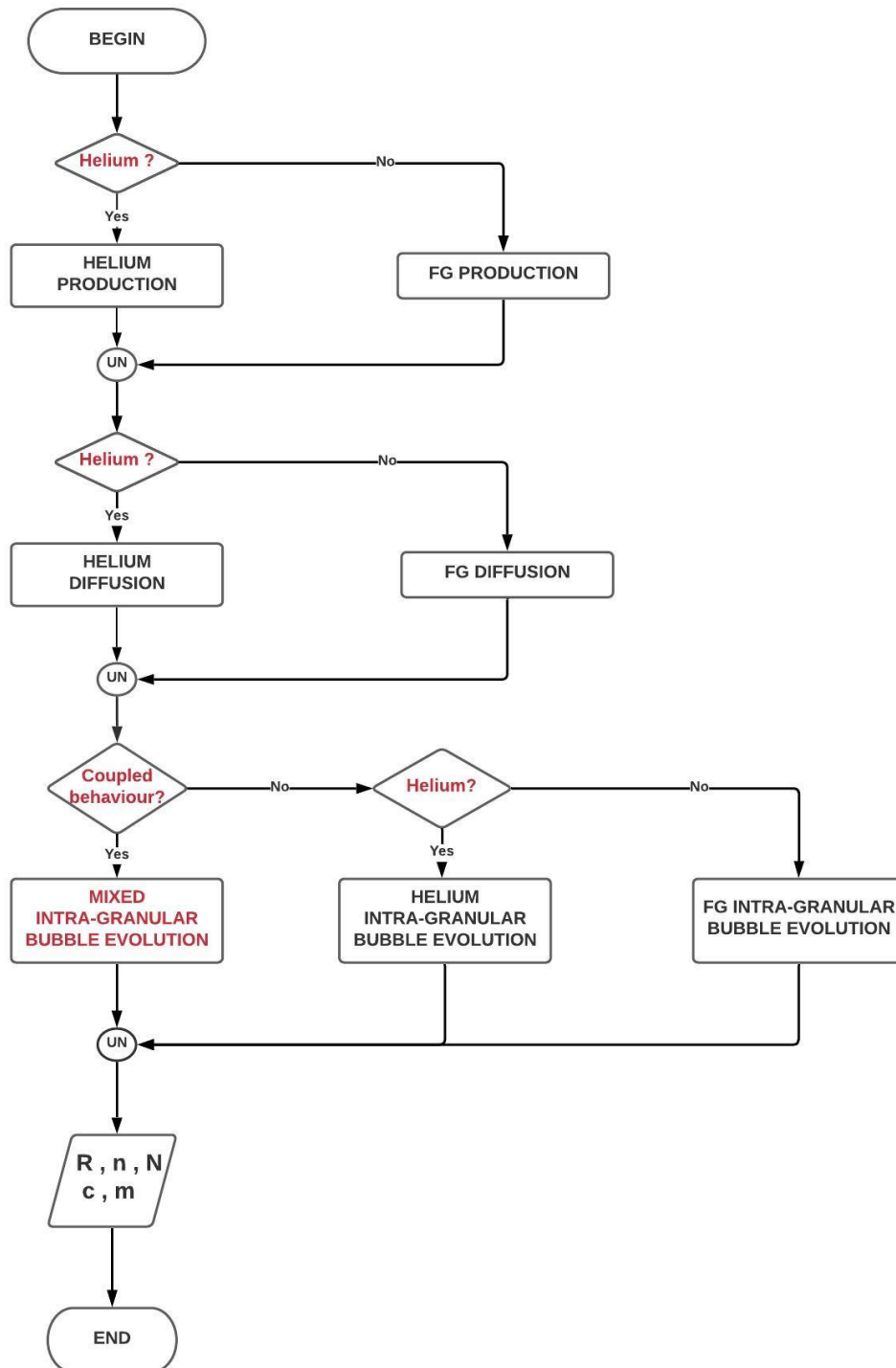
Figure 3.2: Focus on the intra-granular behaviour. The parts highlighted in red have been implemented during this work.

Chapter 4

Model behaviour in annealing conditions

Abstract

This thesis provides a physics-based model that couples inert gas behaviour in the fuel grain and describes the evolution of mixed intra-granular bubbles. It is a first attempt in this field to account for their coexistence in the fuel grain, for this reason experiments on the matter are unavailable. Nevertheless, an experimental program investigating the behaviour of inert gas cocktails in annealing conditions is planned in the frame of different research initiatives. For this reason, in the following pages it is applied a reduced version of the model to reproduce several annealing scenarios starting from two cases of irradiation, respectively at low and high burn-up. They lay the foundation for future experimental investigations on cocktails of inert gases. That is to say, the simulations identify suitable ranges of temperature, gas compositions and gas fractional release that could serve as starting points for the set-up of forthcoming investigations. The structure of the work is based on the division between the low burn-up case (1 week of irradiation) and the high burn-up case (8 years of irradiation). As conclusion, it is proposed a graphical representation of the more promising ranges of investigations in which the model predicts an observable interaction between helium and fission gas in the fuel grain.

4.1   Annealing maps

The validation of the new model against separate effect experiments was impossible in this work due to the lack of experimental data concerning the cocktail of helium and fission gases. To assess the model behaviour, in a way alternative to the comparison with experimental results, several annealing scenarios have been reproduced. These simulations lay the foundation for future experimental investigations on cocktails of inert gases. They enable to identify suitable ranges of gas compositions in the grain, temperature and gas release that could be interesting to explore. The aim is to produce the basis for targeted experiments. In a second phase, the results of these forthcoming investigations could be useful to validate the model and tackle its limitations.

Description of the simulation set-up

The simulations reproduce annealing experiments, for which a simplified version of the model is sufficient. This approach allows to consider one sub-problem involving a limited number of parameters. For example, the irradiation induced re-solution is not taken into account.

The temperature histories are characterized by a heat up step (around 1 h from 300 K up to the final temperature), followed by a holding at the annealing temperature for 20 h. An example of temperature history is proposed in Fig.4.1. The annealing temperatures vary from 1000 K to 2000 K. This range includes the majority of the operational conditions of the fuel in the reactor.

The specific type of simulation involves only some of the processes described in Chapter 2, i.e.:

1. Trapping at intra-granular bubbles;

2. Single gas atom diffusion;

3. Thermal re-solution.

Point 3 implies that only helium atoms can return into the lattice and can do that simply by thermal re-solution. Single gas atoms cannot be knocked back from bubbles into the lattice due to the passage of fission fragments, because the irradiation is not considered. No bubble coalescence is taken into account, so the amount of gas in bubbles can only grow as a result of trapping. Grain growth and the grain boundary sweeping are not included. In addition to this, the gas reaching the grain boundary is instantaneously released. Grain boundaries act as perfect sinks for diffusing gas [38]. Bubbles nucleation happens before the annealing. During the simulations the number of bubbles remains constant, since they nucleate as effect of irradiation.

The starting points of the annealing simulations are two cases of irradiation, respectively at low and high burn-up. The first case considers an irradiation of 1 week (around 240 MWd/t_U), starting from fresh fuel at the beginning of fission gas production. The second case accounts for an irradiation that lasts 8 years (around 100 GWd/t_U). The value of the latter burn-up corresponds to an upper limit for fast reactors. These choices of burn-up allow to consider the regions of interest for fission gases in fast reactors, that is to say the beginning of life after the fuel restructuring
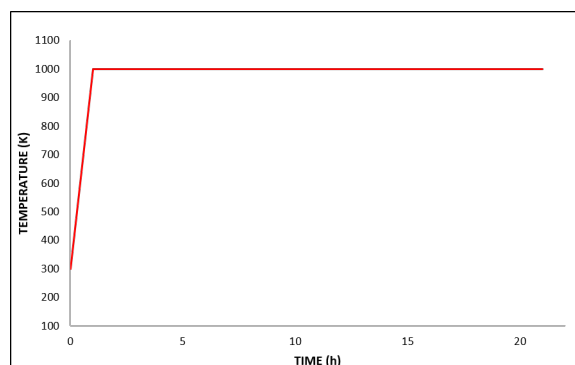

Figure 4.1: Example of idealized temperature history performed in the simulations.

Table 4.1: List of initial values for the parameters adopted in the simulations.

Symbol	Definition	Value	u.o.m	Reference
y_F	Fission yield of xenon and krypton	0.3		
$\dot{F}$	Fission rate density	10^{19}	$m^{-3}\,s^{-1}$	[49]
$M_{M_{Xe}}$	Xenon molar mass	134	$g\,mol^{-1}$	
$M_{M_{He}}$	Helium molar mass	4	$g\,mol^{-1}$	
N_{ig}	Number of intra-granular bubbles	$7\ 10^{23}$	bubbles m^{-3}	[49]
m_{he}	Atoms in bubbles	5% of total helium produced	at m^{-3}	[38]
m_{fg}	Atoms in bubbles	30% of total FG produced	at m^{-3}	Experimental observations
R_{grain}	Grain radius	5	μm	

and the end of life.

The calculations start from the total quantities of xenon and krypton produced during the irradiation time. The helium quantity is obtained varying its weight percentage in comparison to the FG in the cocktail.

Taking into account the irradiation time, the initial quantity of fission gas atoms is calculated as:

$$c_{FG,tot} \text{ (at m}^{-3}) = y_F \dot{F} t \tag{4.1}$$

where y_F is the fission yield of xenon and krypton, $\dot{F}$ is the fission rate density (fissions $m^{-3}\,s^{-1}$) and t is the time (s).

The reference values for each initial parameter are collected in Table 4.1. The fission yield includes the iodine and indirect yields for xenon and krypton. The molar mass of xenon is a representative value for the different isotopes of xenon and krypton. The fission gas mass is derived from equation 4.1 with the formula

$$M_{FG} \text{ (g)} = \frac{c_{FG,tot}\ M_{M_{Xe}}\ V_{grain}}{N_{av}} \tag{4.2}$$

where V_{grain} (m^3) is the grain volume obtained from the grain radius and N_{av} (at mol^{-1}) is the Avogadro's number.

The quantity of helium is varied as follows

$$M_{He} \text{ (g)} = \frac{w_{\%He}}{1 - w_{\%He}} M_{FG} \tag{4.3}$$

where $w_{\%He}$ is the weight percentage of helium in the grain and M_{FG} (g) is the mass of fission gases. The use of the weight percentage allows to take into account the effects related to the different dimensions of the atoms. It is noted that for $w_{\%He}$ equal to one the helium mass goes to infinite. As approximation, in the pure helium case the helium mass corresponds to 1000 times the mass of fission gases.

For each temperature history one figure of merit has been analysed, the gas fractional release. It is measured up to the end of the annealing plateau. The results have been collected for each temperature and weight percentage and plotted in 3-dimensional maps.

It is recalled that the simulations are performed by SCIANTIX, where the model is implemented. The gas fractional release is collected by MATLAB, that builds the plots and allows to visualize the outcomes. In the following sections the results of

the simulations are reported based on the value of the burn-up considered. The goal is to provide a better understanding of the release mechanism for helium and fission gas.

4.2   Low burn-up simulations

As mentioned before, the low burn-up simulations refer to 1 week of irradiation (around 240 MWd/t$_U$). The number of bubbles at the beginning of the annealing tests is 7×10^{22}, lower than the value reported in Table 4.1 to consider the smaller period of time.

- **Helium**
  The plots in Fig.(4.2)-(4.4) describe the fractional release of helium as function of helium weight percentage and temperature. As expected the helium release increases with temperature. For every percentage of helium in the grain the release reaches its maximum after ∼1700 K. At 2000 K the quantity of helium released almost reaches 100%. It means that all the helium atoms trapped at the bubbles have undergone thermal re-solution and diffusion to the grain boundaries. From the plots it could be identified a temperature threshold (hence an activation energy) at which the diffusion to grain boundary starts. It is pointed out the gradient of release with respect to the temperature. Due to the limited number of processes involved in the simulations, it can be expected that the trapping prevails before the beginning of the release slope, after this threshold the diffusion process and then the thermal re-solution take over. At high temperatures it could be said that the thermal re-solution comes in promoting the release until its maximum. This could be the reason why the release of helium is 1000 times higher than the FG release. The fission gases in fact are not influenced from the thermal re-solution as mentioned in chapter 2, hence when an atom of FG is trapped at the bubble cannot re-enter the grain solution. Figure 4.3 shows that the quantity of helium released decreases as the weight percentage of helium increases. The fractional release is almost constant in temperature before 80% of helium, after this value the lines start bending. This behaviour could point out an interaction between helium and FG in the grain, which in turn in the model has an influence on the bubbles radius. The bubble radius is strongly affected by the presence of fission gases, their dimension is in fact large compared to helium dimension. This effect is likely to be one cause of the line curvature together with the increasing quantity of helium in the grain. The large quantity of helium could promote the trapping process over the thermal re-solution. In this regard, it can be noted that with a high helium percentage the threshold of maximum release moves at temperatures higher than 1700 K.

- **Fission gas**
  As for the case of helium, in Figures 4.5-4.7 the gradient of release and the temperature threshold at which the release starts can be identified. This is also the point at which the diffusion prevails on the trapping process. It is recalled that the solubility of fission gases is neglected. For this reason the gas in the solution has a possibility to reach the grain boundary only by diffusion, the gas initially trapped at the bubbles cannot move. From here the low quantity of fission gas released with respect to the helium case.
  The different behaviour of the fission gases is reflected in the plateau of max-

imum release, which is limited to a small range of temperatures and does not include the maximum temperature of 2000 K. After 1800 K the release decreases, it could mean that again the trapping prevails. At high temperatures the atoms diffusing could have more chances of being trapped than released, from here the negative slope. On the other side, the reason why helium does not produce the negative slope is ascribed to the presence of the thermal re-solution. The thermal re-solution could compensate the trapping process avoiding the same behaviour of FG.

The gas fractional release decreases proportionally to the FG percentages ($w_{\%FG}$) in the cocktail. Figure 4.6 shows a clear change in the behaviour of FG at low weight percentages, complementary to the helium behaviour at high percentages. It is expected that the massive presence of helium reduces the total gas reaching the grain boundary. The small quantity of fission gas initially in the solution is more likely to be trapped at the bubbles than released at the grain boundaries.
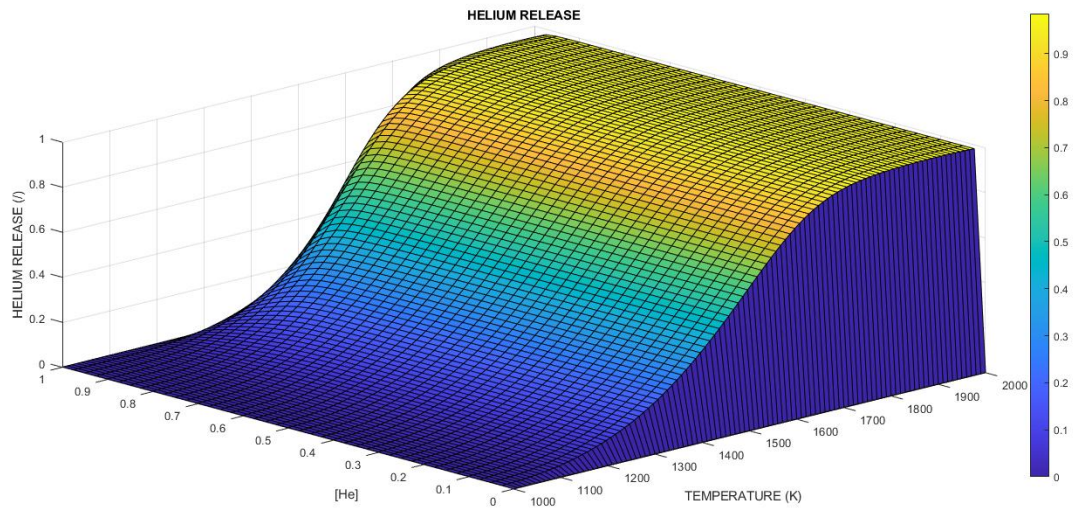
Figure 4.2: 3D plot of helium fractional release at low burn-up (240 MWd/t$_U$).
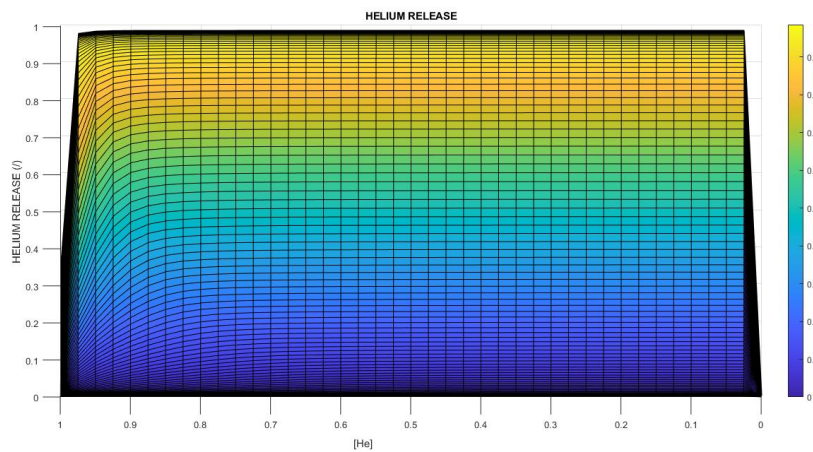

Figure 4.3: View 1 of the helium fractional release plot at low burn-up.
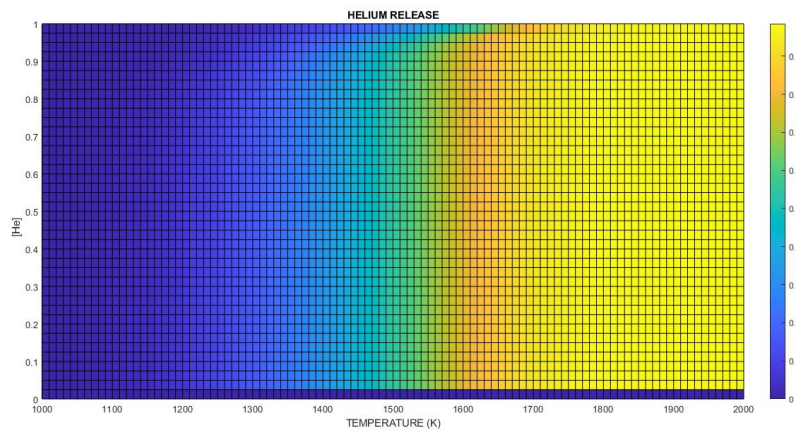

Figure 4.4: View 2 of the helium fractional release plot at low burn-up.
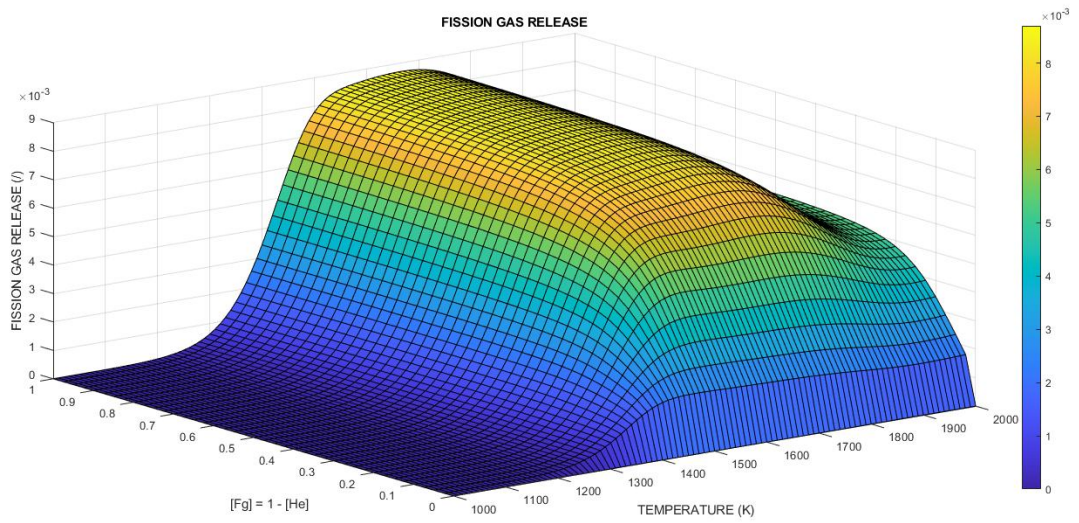
Figure 4.5: 3D plot of FG fractional release at low burn-up (240 MWd/t_U).
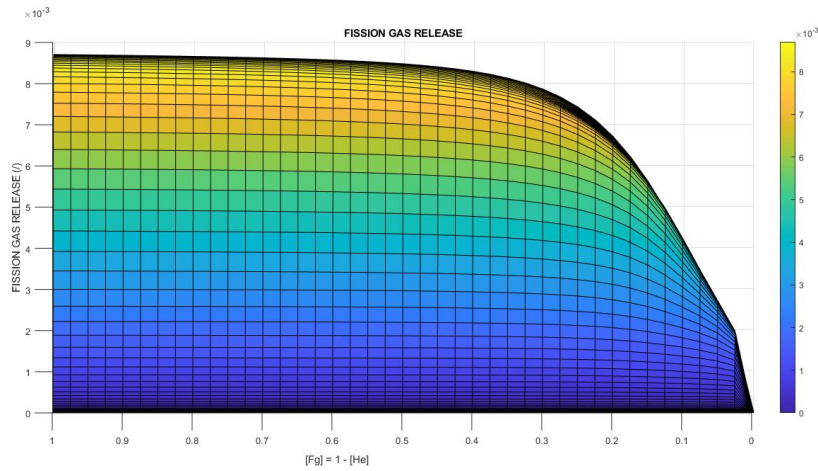
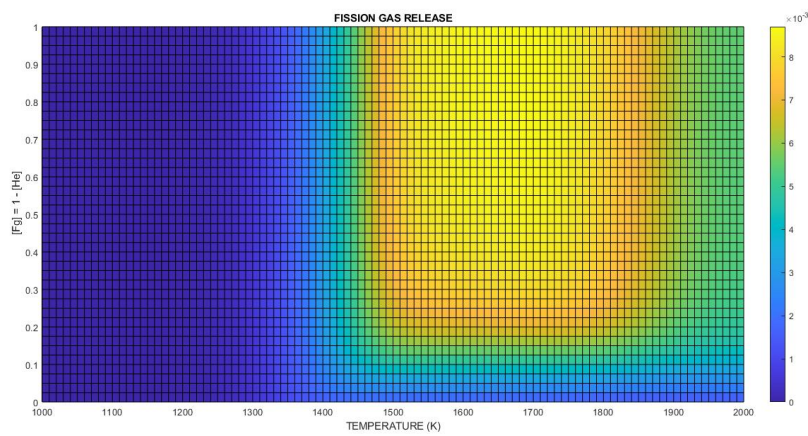Figure 4.6: View 1 of the fission gas fractional release plot at low burn-up.

Figure 4.7: View 2 of the fission gas fractional release plot at low burn-up.

4.3 High burn-up simulations

The high burn-up simulations refer to 8 years of irradiation (around 100 GWd/t$_\text{U}$). The quantity of gas in the grain is higher than the low burn-up case, hence the plots show some differences.

- **Helium**
  The presence of a large quantity of gas in the grain could lead to the conclusion that the fractional release is higher than the low burn-up case. Actually the plots deny this assumption as shown in Figure 4.8 and 4.11. Despite the high temperatures, it is not expected a large release when there is such a big quantity of gas in the cocktail, even less if the cocktail mainly consists of helium. In the case of high percentages of helium, the gas tends to stay in the grain rather than diffuse to the grain boundary. At high burn-up, thermal re-solution and diffusion towards the grain boundary have an evident effect just at low helium percentages and high temperatures. The trapping process prevails all over the plots, this could be due to the higher number of atoms and bubbles with respect to the previous case. The atoms in the grain solution on their way towards the grain boundary could have more chances to meet a bubble trap, hence the lower release. However, it can be said that there is an interaction between the atom species. This conclusion comes from the consideration that the helium fractional release has a continuous decrease as its weight percentage in the cocktail is varied (Fig. 4.9).

- **Fission gas**
  Differently from the helium case, Figure 4.13 shows a threshold of release around 1200 K for every weight percentage of fission gas. After this temperature threshold, it is evident the variation in the FG release (Fig. 4.12). It is recalled that the quantity of fission gas remains constant across all the simulations at high burn-up, for this reason it can be stated that this effect is a consequence of the interaction with helium. Consistently with the low burn-up case, the quantity of fission gas reaching the grain boundary is much lower than helium values, in this case is 10000 times lower. The cause is again the fact that the irradiation induced re-solution is neglected and that the FG atoms once trapped at the bubbles cannot escape. The negative slope of release at high temperatures is outlined just at high FG weight percentages, in other regions of the plot is not clear. This means that the presence of helium not only influences the FG release but also its trend with respect to the temperature. That is to say, comparing the fission gas release as function of temperature, at high percentage a maximum release is shown at 1500 K while at low percentages the release reaches a plateau. The peculiar behaviour at high gas percentages required a more in depth study of the simulations. It can be concluded that the temperature of 1500 K corresponds to an optimal value for the fission gas release, which is interesting from different points of view. The main considerations concern the physical processes involved. At 1500 K the trapping process is compensated by a strong diffusion that helps the re-

lease. Before 1500 K the trapping is lower but the diffusion process has not the necessary strength to move the atoms until the grain boundary. After 1500 K despite the strong diffusion the trapping process prevails, because the atoms are trapped in the first hour of annealing and as already said, once trapped the atoms cannot escape. At low weight percentages of gas in the cocktail this behaviour is no more evident. When the atoms start diffusing, the processes of trapping and diffusion compensate each other maintaining almost a constant release.
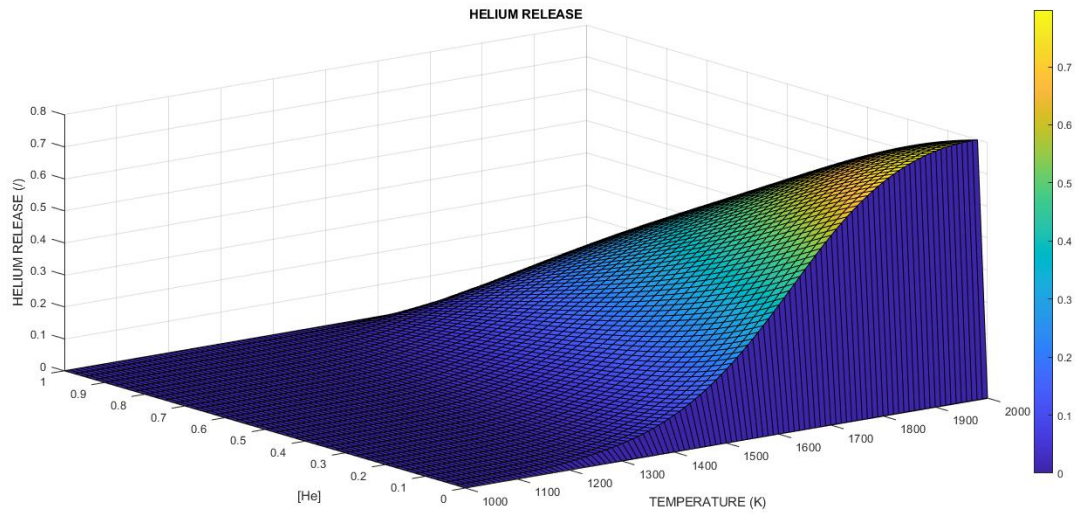
Figure 4.8: 3D plot of helium fractional release at high burn-up (100 GWd/t_U).

Figure 4.9: View 1 of the helium fractional release plot at high burn-up.

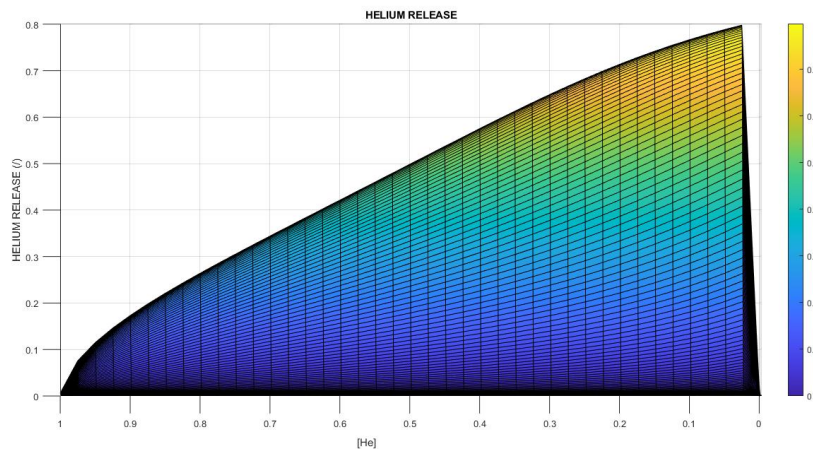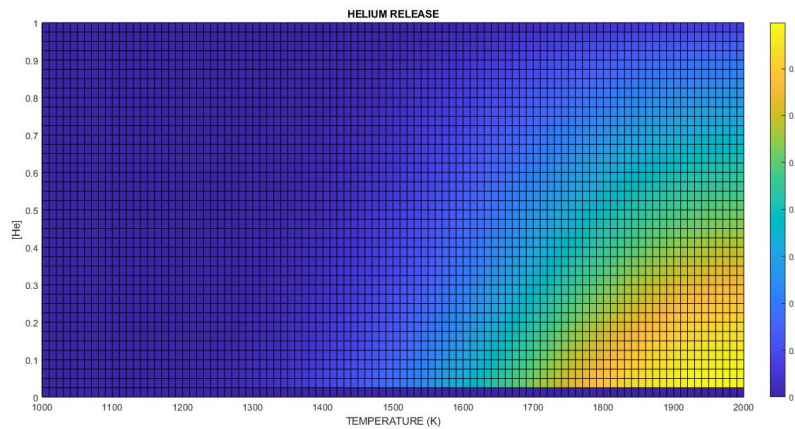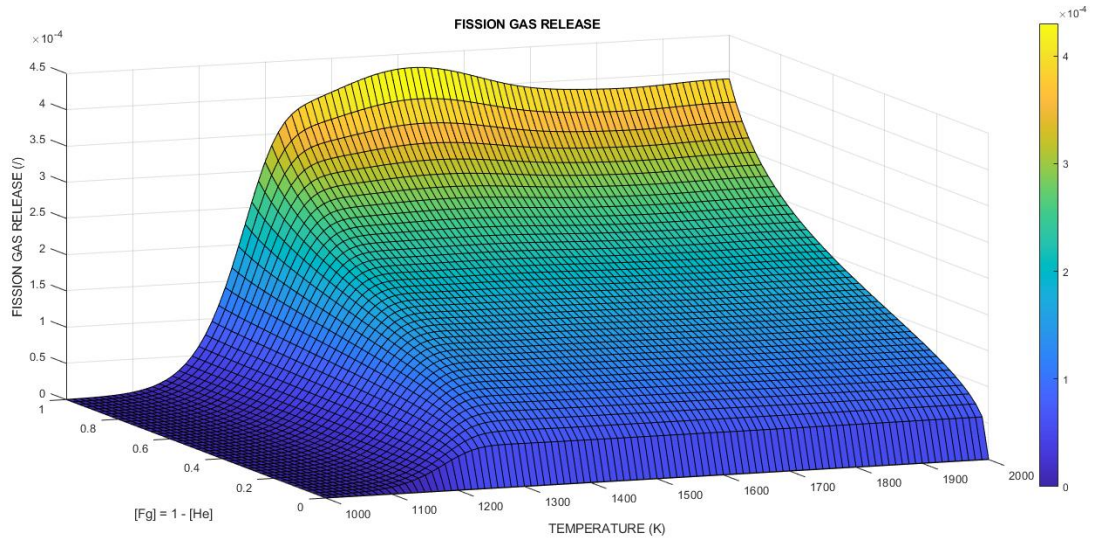Figure 4.10: View 2 of the helium fractional release plot at high burn-up.

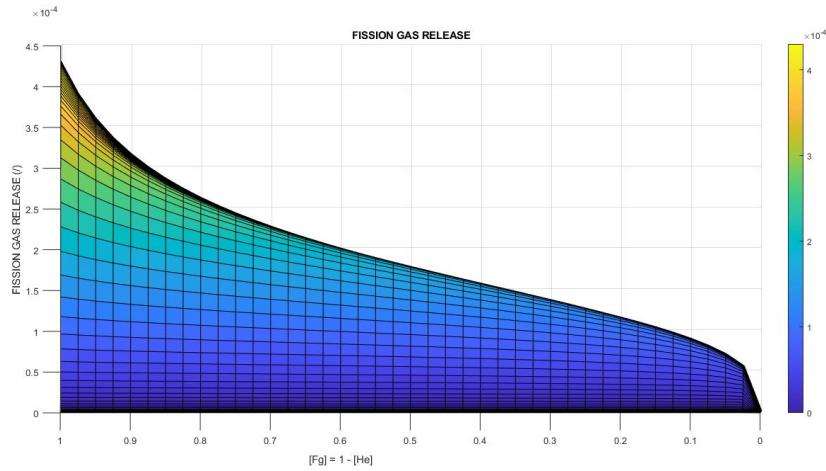Figure 4.11: 3D plot of fission gas fractional release at high burn-up (100 GWd/t$_U$).

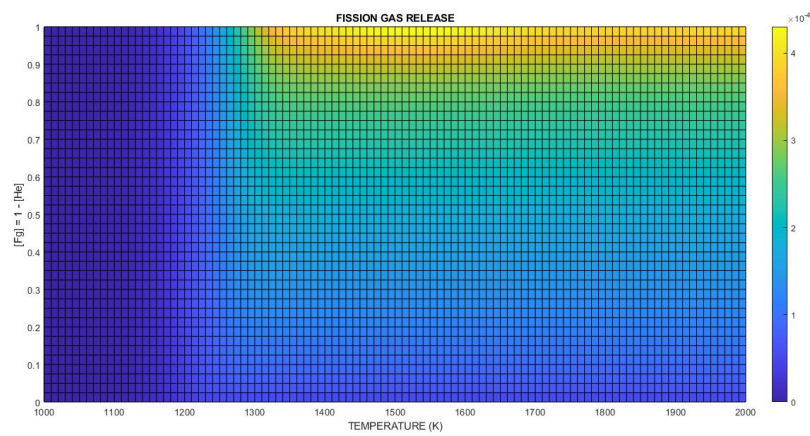Figure 4.12: View 1 of the fission gas fractional release plot at high burn-up.

Figure 4.13: View 2 of the fission gas fractional release plot at high burn-up.

4.4 Discussion of results

The aim of these simulations is to test the model in annealing conditions and to find combinations of inert gases in which is likely to observe an interaction between the atom species. The resulting plots suggest possible temperature ranges and gas combinations that could serve as starting points for the set up of future experiments. Figure 4.14 highlights in white the regions of interest at low and high burn-up, taking into account the observations of the previous sections. The plots correspond to Figure 4.4, 4.7, 4.10 and 4.13. The top figures are mirrored with respect to the bottom figures in order to easily identify the cocktail composition. From the left to the right, at low burn-up it is suggested a cocktail of inert gases made at 50% of helium and 50% of fission gases. This combination allows to identify the gradient of release that varies with the temperature and the threshold at which the diffusion starts. Another attractive region of study at low burn-up could be the one with an high weight percentage of helium and a low percentage of fission gases. This combination is the more promising to identify an interaction among the gases according to the model. As the previous plots suggest, the massive presence of helium in the cocktail evidently affects the fission gas release, highlighting an interaction of the gases in the grain. In addition, the positions of the rectangles point out the areas of maximum release, in order to outline the relative weight of the trapping process with respect to diffusion and thermal re-solution. The rectangle on the plot of fission gases covers high temperatures to include the negative slope of release and highlight the confined plateau. This part of the plot is attractive because the model outlines a range of maximum release that does not include the highest temperatures as it was expected instead.

At high burn-up the entire range of gas composition would be interesting, because of the different shapes of the plots. The release of both helium and fission gases changes continuously varying the weight percentages. However, it could be preferable to choose a cocktail made by a large quantity of one atom specie with respect to the other, as pointed out in Figure 4.14. Differently from the low burn-up case, the region of maximum release is not continuous but it is limited to high temperatures and low quantities of helium. The trapping process in fact has the largest weight in the simulations. For this reason, the diagonals highlight the gradient of release and the regions of maximum release expected. The last rectangle on the right is positioned to outline that, despite the high temperatures, the expected release is not so high. The rectangle also suggests to investigate the gas behaviour when a large quantity of helium is in the grain, because it is the region where an interaction between the gases could be meaningful.

The following chapter further examines these results focusing on the parameters that impact on the model. The sensitivity analysis could support the observations proposed so far.
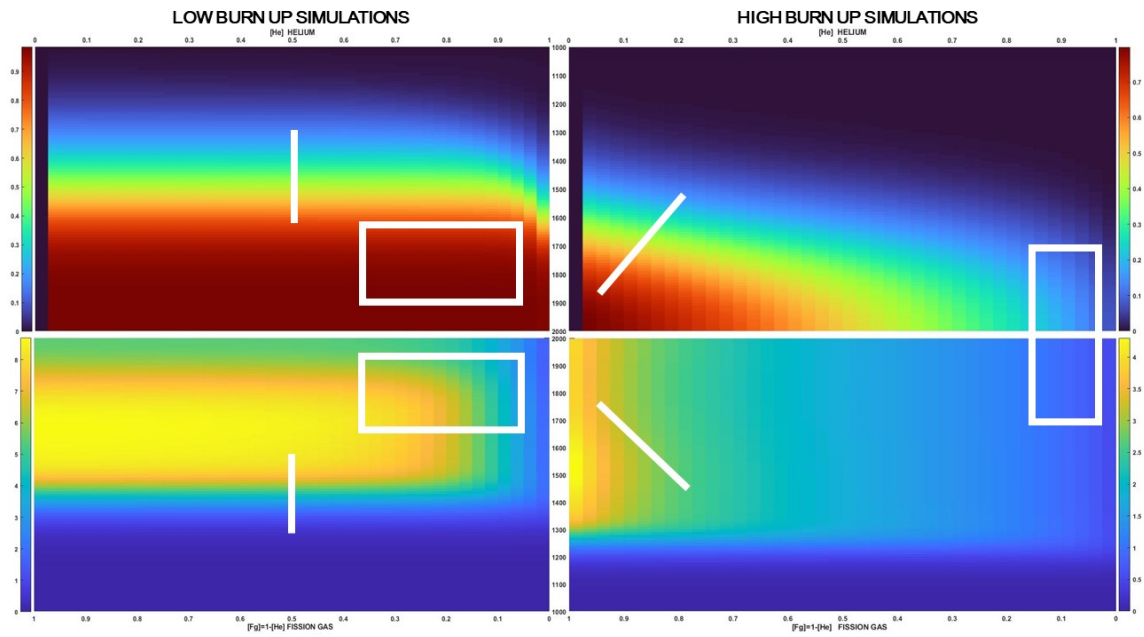
Figure 4.14: Mirrored view of low and high burn-up simulations. The white lines highlight the suggested ranges of investigation. The colour bars on the external sides indicate the quantity of gas fractional release. The axes at top and bottom specify the weight percentages of helium and fission gas, respectively. The vertical axis in the center corresponds to the temperature.

Chapter 5

Sensitivity analysis

Abstract

Referring to the annealing simulations of the previous chapter, it is performed a sensitivity analysis with the Pareto method quantifying the impact of the uncertainties in the model parameters (helium and fission gas diffusion coefficient, compressibility factor, Henry's constant) on the model behaviour. The aim of this analysis is to support the results of the annealing simulations. Furthermore, the outcomes limit the efforts of future researches to the study of a particular parameter in the attempt to improve the model predictive capability in annealing as well as in irradiation conditions. The diffusion coefficients and Henry's constant turn out to have the major influence on the model behaviour. This result was in part expected and it is justified by the processes involved. The compressibility factor occupies the last position across all the simulations, leading to the conclusion that the related helium pressure does not have a big relevance in the development of the model compared to other parameters.

5.1   Pareto method

As conclusion to the annealing simulations, a sensitivity analysis is conducted on few parameters of the model using the Pareto method. Up to a certain degree, it is expected that adding physics-based parameters with considerable uncertainty [8, 17, 31] results in a limited predictive capability of the model itself. For this reason the aim of the analysis is to identify the parameters whose uncertainties have the

Table 5.1: Scaling factors for the Pareto analysis

Symbol	Definition	Lower bound	Upper bound	Reference
D_{he}	Helium diffusion coefficient	0.1	10	[17]
D_{fg}	FG diffusion coefficient	0.1	10	[20]
k_{henry}	Henry's constant	0.001	1000	[8]
Z_1	Compressibility factor	0.9	1.5	-
Z_2	Compressibility factor	0.1	10	-

major impact on the model. By performing a Pareto analysis, the outcomes can be used to focus attention on the parameters that are contributing the most to the model and limit the efforts to the improvement of a particular uncertainty range. Considering the limited number of physical processes included in these simulations, four parameters are selected as the most representative of the model behaviour: helium diffusion coefficient (D_{He}), FG diffusion coefficient (D_{FG}), Henry's constant (k_H) and the compressibility factor (Z).

Each parameter is described by a suitable correlation which brings along its own uncertainty. It is set a lower bound and an upper bound of uncertainty based on previous experimental studies. Table 5.1 lists the mentioned parameters with the assigned range of uncertainty and the reference study. It is noted that the compressibility factor Z hasn't a citation, its scaling factors are in fact arbitrary. This choice comes from the observation that in the literature there are no clear references about its uncertainties. Hence the use of two ranges for Z, to investigate in more detail its effect on the model. The first range assumes that the base case corresponds to Z equal to one, i.e. ideal gas behaviour. From the study of Van Brutzel [42], it can be deduced that the deviation of helium from the ideal behaviour leads with more probability to Z higher than one instead of Z lower than one. Hence the choice of the uncertainty range. The second range is put equal to the uncertainties of the diffusion coefficients with the aim of evaluating on equal terms which parameter produces the biggest deviation from the base case. The range of Henry's constant was too high to be applied without any further information on Z. However the results obtained from these ranges have been considered sufficient to draw a satisfying conclusion.

The simulations of Section 4.1 are reproduced for each parameter varying the scaling factors. It is maintained the same separation between high and low burn-up, but the cases of pure helium and pure fission gases are excluded since the interest of the study is on the mixed behaviour.

The Pareto chart is a bar chart representing, in this case, the metric of comparison based on the gas release fraction variation due to the upper and lower limits of the considered parameter. For each simulation, the values of the gas fractional release (separately for helium and fission gas) are collected in three different matrices: M_{min} is the matrix corresponding to the simulation with the smallest scaling factor, M_{max} is referred to the highest scaling factor and M is the matrix with scaling factor equal to one. As measure of the modified gas behaviour, the metric is calculated as follows

$$E_{min} = \frac{|M_{min} - M|}{M} \times 100 \tag{5.1}$$

$$E_{max} = \frac{|M_{max} - M|}{M} \times 100 \tag{5.2}$$

where E_{min} is the metric with respect to the lower bound and E_{max} is the metric with respect to the upper bound. The value reported in the Pareto chart is the mean of the latter metrics:

$$E_{Pareto} = \frac{\overline{E_{min}} + \overline{E_{max}}}{2} \tag{5.3}$$

where $\overline{E_{min}}$ is the average of matrix E_{min} and $\overline{E_{max}}$ is the average of matrix E_{max}. The goal of the procedure is to understand which parameter has the major influence in general terms, for this reason the sensitivity analysis does not go into further details.

5.2 Discussion of the charts

The presentation of the charts is based on the mean variations in the results with respect to the base case (scaling factor equal to one), they are ordered from the greatest to the lowest value. The bars correspond to the value of the metric for each parameter, the line graph is the cumulative total, the right vertical axis is the cumulative percentage.

- **Low burn-up**
  Figures 5.1 and 5.2 report the Pareto charts for the simulations at low burn-up with Z_1 and Z_2, respectively. In the helium case, the parameter with the largest impact is the helium diffusion coefficient. This analysis reiterates what can be already seen from Figure 4.2 and verifies what can be deduced from the mathematical formulation of the processes. The diffusion coefficient has the main role for the majority of the plot with the trapping at low temperatures and the combination of thermal re-solution and diffusion at high temperatures. The helium diffusion coefficient in fact is part of the formulas describing all the three processes involved. The helium fractional release reaches almost 100% at low burn-up, for this reason a small variation in the diffusion coefficient greatly influences the quantity of helium released and the temperature threshold at which the release becomes significant.
  The second main parameter is Henry's constant, representative of the thermal re-solution process. Recalling that just the 5% of helium atoms is initially trapped at the bubbles and assuming that during the annealing not all the helium atoms in the grain solution are stuck at these traps, it is reasonable that Henry's constant has the costarring role on the scene. Besides, its high uncertainty range made its influence on the model predictable. On the contrary, the effect of thermal re-solution on the fission gas behaviour was not obvious. Figures 5.1b and 5.2b shows that the impact of Henry's constant on the plots even if limited, in comparison to the diffusion coefficient, is not negligible. It means that helium solubility affects the behaviour of the other gases in the grain solution. In particular a negative or positive variation in the thermal re-solution implies a proportional variation in the overall fission gas released. That is to say, if the thermal re-solution decreases it is expected that the bubble radius increases, promoting the trapping process and as consequence affecting the gas release.
  As foreseen the helium diffusion coefficient has a minimal impact on the FG behaviour and vice versa. The diffusion process in fact does not take into account the gas atom interactions in the grain solution.
  It can be noted that the compressibility factor Z has negligible consequences on the model in both its uncertainty ranges (with respect to the gas fractional release). This implies that the choice of the equation of state is not the main concern in the formulation of the thermal re-solution compared to Henry's constant. As a result, the exploration of the best EOS is not the priority at these stages of the model development. Clearly, the increase in the range of Z would lead to different conclusions but the lack of information makes these

results acceptable.

- **High burn-up**

  Figures 5.3 and 5.4 represent the high burn-up case, again with Z_1 and Z_2. In the plots of helium, Henry's constant and the diffusion coefficient switch positions with respect to the previous case. The interpretation of this result requires a callback to the annealing simulations at high burn-up of chapter 4. In Figure 4.8 it is evident that the overall helium fractional release decreases due to the presence of a higher quantity of atoms in the grain. It is deduced that the trapping prevails over the other processes for most of the simulations. This would lead to say that the diffusion coefficient (related to the trapping) is the dominant parameter in the high burn-up case. On the contrary, in the Pareto charts Henry's constant results the most relevant with more than the 80% on the cumulative percentage. Assuming that the majority of the atoms is trapped at the bubbles, the variation in the thermal re-solution is more effective in this case than in the low burn-up case. The quantity of gas released is strongly influenced as consequence of the large variation of Henry's constant. As mentioned before, Henry's constant has an impact on the fission gas behaviour too. Following the same logic, in Figure 5.4b the weight of Henry's constant on the distribution is higher than before. However, coherently with the physics of the process the FG diffusion coefficient is always the first parameter. Z remains the less relevant across all the simulations.

To summarize at low burn-up the diffusion coefficient prevails both for helium and fission gas followed by the effect of Henry's constant. This result was predictable from the plots of chapter 4 and from the fact that the diffusion coefficient is adopted for the mathematical description of all the processes involved.

At high burn-up the trapping process prevails, but differently from what expected Henry's constant has the major impact on the model in the case of helium. The reasons could be the low quantity of helium released susceptible to the variation in the thermal re-solution and the high range of uncertainty. The fission gas diffusion coefficient always influences the most the FG simulations.

Z is the least important in both its uncertainty ranges. This behaviour can also be ascribed to the poor characterization of the parameter. Since the equation of state is directly related to Z (Section 3.3), its formulation does not have a big relevance in the development of the model. From here the choice of not investigating other types of EOS in this thesis.

In conclusion it is questioned the effect of the model parameters on the model behaviour under irradiation conditions. The distribution of the relative weight of the parameters on the figure of merit is expected to change. Due to the presence of the fission fragments, the nucleation rate and the irradiation induced re-solution rate cannot be neglected. It is foreseeable that the irradiation induced re-solution predominates on the thermal re-solution since it has an effect on both helium and fission gas. Considering the work of Pizzocri et al.[30] and the uncertainty ranges adopted for the nucleation rate and the re-solution rate, it can be expected that

the dominant parameter on the gas release remains the diffusion coefficient. The mentioned work states that the trapping rate (hence, the gas atom diffusion coefficient) has the main role in the irradiation experiments considered. Even if [30] refers to the intra-granular bubble swelling as figure of merit, this consideration could be extended to the release case.

New experiments tailored on these parameters would be of great interest to reduce their uncertainties and to improve the model predictive capability in annealing as well as in irradiation conditions.

(a) Pareto chart 1 for helium.

(b) Pareto chart 1 for fission gas.
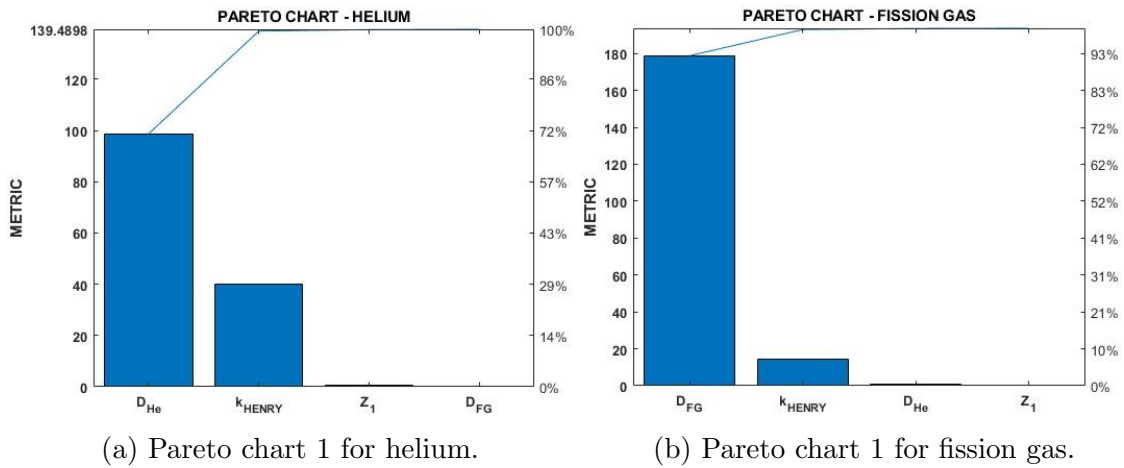
Figure 5.1: Pareto charts at low burn-up with Z_1.

(a) Pareto chart 2 for helium.

(b) Pareto chart 2 for fission gas.
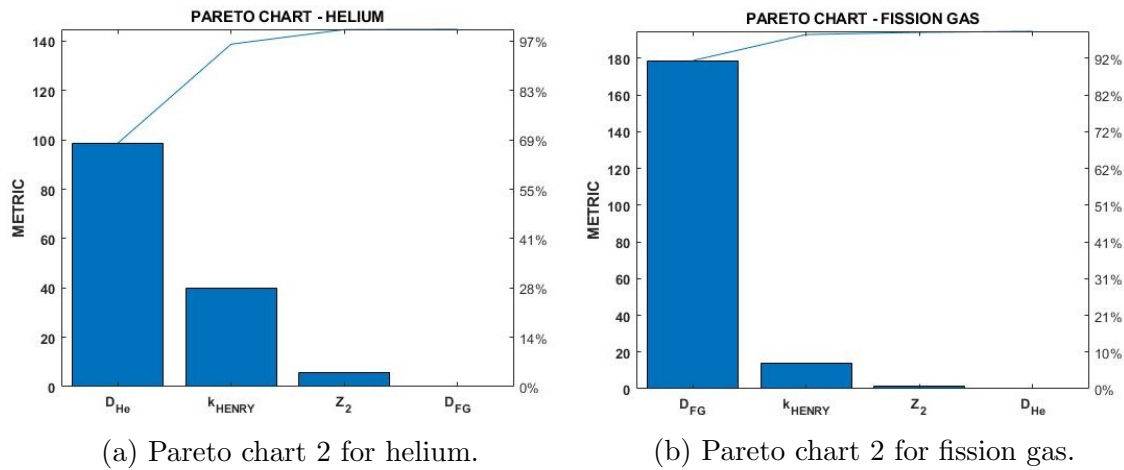
Figure 5.2: Pareto charts at low burn-up with Z_2.

(a) Pareto chart 3 for helium.

(b) Pareto chart 3 for fission gas.
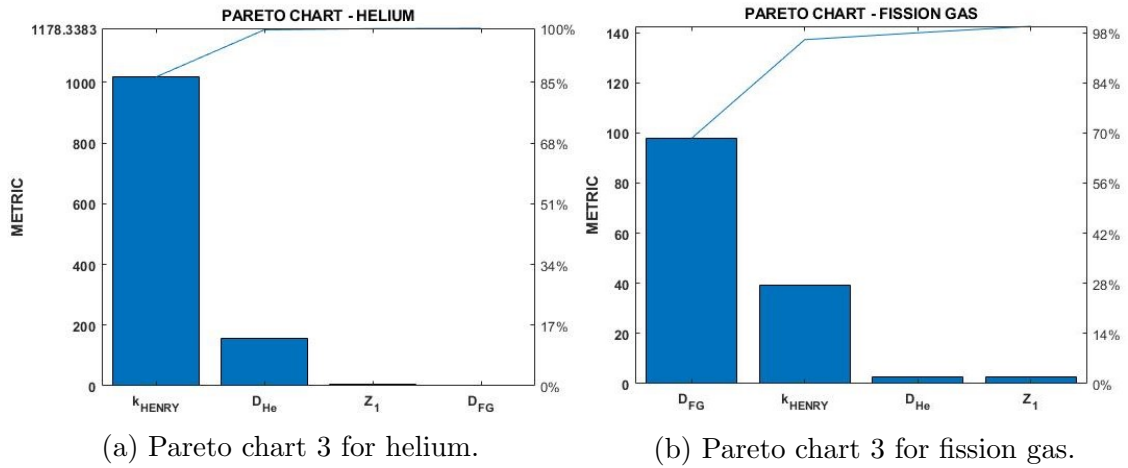
Figure 5.3: Pareto charts at high burn-up with Z_1.

(a) Pareto chart 4 for helium.

(b) Pareto chart 4 for fission gas.

Figure 5.4: Pareto charts at high burn-up with Z_2.

Chapter 6

Conclusion

This thesis work represents a first attempt to address the coupled intra-granular behaviour of a cocktail of inert gases. The state-of-the-art modelling resorts to separate models for the evolution of helium and fission gases in the fuel grain. This is the starting point of the work. The model in fact comes from the synergy of two different studies involving helium and fission gas separately. It describes their coexistence in intra-granular bubbles still retaining a physical basis. The processes characterizing the model are the classical processes of single gas atom diffusion, bubble nucleation, re-solution into the lattice and gas atom trapping at the bubbles. The inclusion of helium calls for the necessity to consider its solubility with the use of a suitable equation of state. In this regard, it is made a distinction between irradiation induced and thermal re-solution.

The work heads to the simulations of several annealing scenarios in order to accelerate the process of design and realization of experiments that could produce useful data for the validation of the model. The aim of this study is to identify suitable ranges of gas compositions in the grain, temperature and gas release that could be interesting to explore in future experimental investigations. The role of these simulations is to provide a basis to customize forthcoming experiments on cocktails of inert gases. Furthermore, the onset of the physical processes involved (trapping, diffusion and thermal re-solution) can be distinguished shedding light on their regions of predominance. The results allow to say that the massive presence of helium in the cocktail evidently affects the fission gas release. The quantity of helium is so high that their reciprocal influence in the grain cannot be neglected.

In order to support the annealing simulations it is performed a sensitivity analysis based on the Pareto method. Focusing on four model parameters (diffusion coefficient, compressibility factor, Henry's constant) it is analysed the impact of their uncertainties on the model results. It can be assessed that the parameters to which the model is susceptible the most are the diffusion coefficients and Henry's constant. The latter was expected to emerge due to its high uncertainty range. On the other side, the diffusion coefficients are part of the formulations of all the processes involved, so their impact is justifiable. These outcomes can limit the efforts of future researches to the study of a particular parameter in the attempt to improve the model predictive capability in annealing as well as in irradiation conditions.

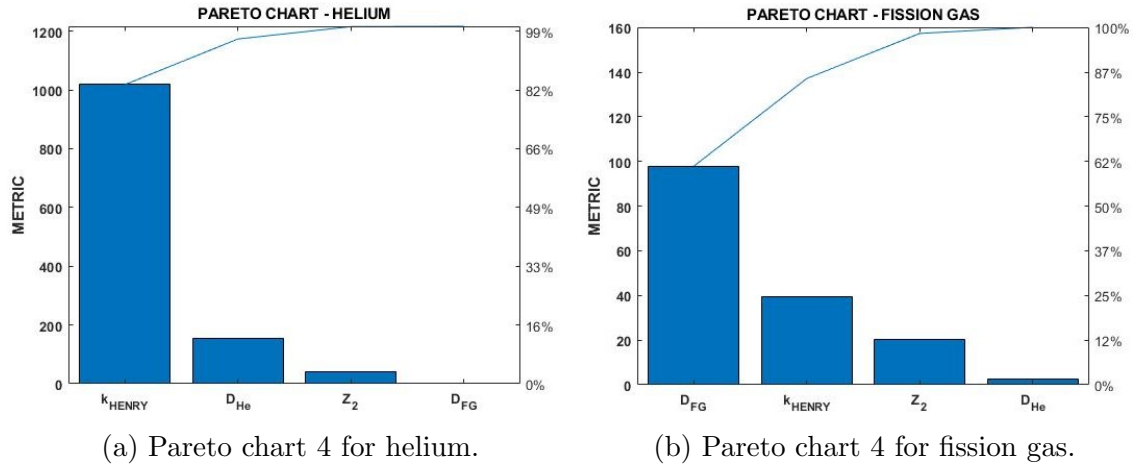An experimental program investigating the behaviour of inert gas cocktails in an-

77

nealing conditions is planned in the frame of different research initiatives. As soon as the results of these experiments will become available, the validation of the model can be foreseen. In addition to this, new experiments could be of great interest to reduce the uncertainties of model parameters such as Henry's constant and the diffusion coefficients and to fill the lack of data concerning the related physical processes. To another level, the next steps of the work could involve the extension of the model to the inter-granular behaviour. Intra-granular gas diffusion to grain boundaries in fact provides the source term for the inter-granular processes, ultimately leading to grain-boundary gaseous swelling and fission gas release.

Lastly, the validation of the model against integral irradiated fuel rod experiments could be interesting in perspective. This would require a more in depth study of the weight factors describing the mechanisms of irradiation induced re-solution in the model.

Appendix A

Equations Verification

The aim of the present Appendix is to verify the system of equations introduced in chapter 3. The following balance equations clarify the accuracy of the model and prove that the total number of gas atoms is preserved. It is recalled that $m = nN$.

Balance on the total gas atom concentration in bubbles and in solution:

$$\left(\frac{\partial c_{FG}}{\partial t} + \frac{\partial m_{FG}}{\partial t} \right) + \left(\frac{\partial c_{He}}{\partial t} + \frac{\partial m_{He}}{\partial t} \right) =$$
$$= S_{FG} + D_{FG}\nabla^2 c_{FG} + (-g_{FG} + g_{FG})\, c_{FG} + (b_{FG} - b_{FG})\, m_{FG} + (-\nu + \nu)\, n_{FG} +$$
$$+ S_{He} + D_{He}\nabla^2 c_{He} + (-g_{He} + g_{He})\, c_{He} + (b_{He} - b_{He})\, m_{He} + (\gamma - \gamma)\, m_{He} + (-\nu + \nu)\, n_{He} =$$
$$= S_{FG} + S_{He} + D_{FG}\nabla^2 c_{FG} + D_{He}\nabla^2 c_{He}$$

$$(A.1)$$

Balance on helium and fission gas atoms in bubbles (at m^{-3}):

$$\frac{\partial (m_{FG} + m_{He})}{\partial t} = \frac{d\left(N(n_{He} + n_{FG})\right)}{dt} = N\frac{dn_{He}}{dt} + N\frac{dn_{FG}}{dt} + (n_{He} + n_{FG})\frac{dN}{dt} =$$
$$= (g_{He}c_{He} - b_{He}m_{He} - \gamma m_{He} + \nu n_{He}) + (g_{FG}c_{FG} - b_{FG}m_{FG} + \nu n_{FG}) =$$
$$= \frac{\partial m_{He}}{\partial t} + \frac{\partial m_{FG}}{\partial t}$$

$$(A.2)$$

Balance on helium atoms in bubbles (at m^{-3}):

$$\frac{\partial m_{He}}{\partial t} = \frac{\partial(N\,n_{He})}{\partial t} = N\left(g'_{He}c_{He} - b'_{He}n_{He} - \gamma n_{He}\right) + n_{He}\left(\nu - b''N\right) =$$
$$= g_{He}c_{He} - (b'_{He} + b'')m_{He} - \gamma m_{He} + \nu n_{He}$$

$$(A.3)$$

Balance on fission gas atoms in bubbles (at m^{-3}):

$$\frac{\partial m_{FG}}{\partial t} = \frac{\partial(N\ n_{FG})}{\partial t} = N\left(g'_{FG}c_{FG} - b'_{FG}n_{FG}\right) + n_{FG}\left(\nu - b''N\right) =$$
$$= g_{FG}c_{FG} - (b'_{FG} + b'')m_{FG} + \nu n_{FG} \tag{A.4}$$

Appendix B

Verification of the helium path in SCIANTIX

After the implementation of the coupled path for inert gases in SCIANTIX, the work did not proceed directly to the verification of the new model. Prior to this step, the effective capability of SCIANTIX to handle the mixed as well as the separated gas behaviour has been tested. For this purpose, the single path for helium has been verified reproducing part of the work of Cognini et al.[7], which in turn is based on the experiments performed by Talip et al.[38]. The fission gas path has been checked too, but it is not reported since its verification is identical to the helium case.

Therefore the aim of this section is to prove that the present work has not modified the previous capacities of the SCIANTIX code. On the contrary, it will be shown that it has added an independent way to describe the behaviour of combined gases in fuel grains.

Description of the simulations and results

The simulations reproduce fast annealing experiments performed in vacuum conditions [38]. The model proposed and adopted in the simulations is different from the one presented in this thesis. It describes the intra-granular helium behaviour neglecting the fission gas.

The helium model includes single-atoms diffusion, trapping of single atoms at intra-granular bubbles and irradiation induced re-solution of gas atoms from intra-granular bubbles, helium solubility, and helium production rate. For a more detailed explanation of model and experiments refer to Ref.[7, 9].

Table B.1: Initial conditions of the fast annealing simulations.

Symbol	Definition	Value	u.o.m
c_{He}	Single atoms in grain	$1.6 \ 10^{24}$	at m^{-3}
m_{He}	Atoms in bubbles	$8.3 \ 10^{22}$	at m^{-3}
N_{ig}	Bubble density	$2.08 \ 10^{20}$	bubbles m^{-3}
n_{He}	Atoms per intra-granular bubble	400	at bubble^{-1}
R	Bubble radius	1	nm

As consequence of the experimental set-up, the irradiation induced re-solution rate is null and helium production rate is neglected due to the fast transients. It is assumed that a bubble population is formed at the first time-step and then it evolves during the whole experiment. The initial conditions of the simulations are reported in Table B.1. The grain growth and the consequent grain boundary sweeping are taken into account.

Five annealing temperature histories are considered (Fig.B.1) and are characterized by a heat up step, followed by a holding at the annealing temperature (for 1-3 h). In three of them, the temperature is decreased after the plateau, while in two histories there is a second heat up phase up to 2200-2300 K.
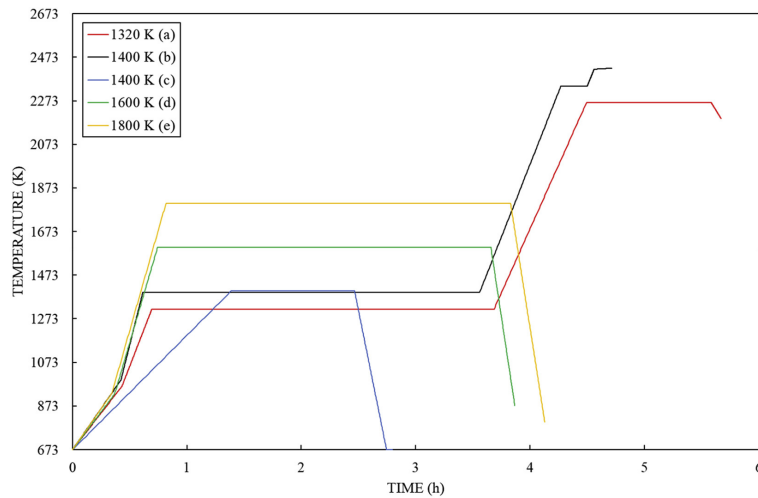

Figure B.1: Temperature histories of the annealing experiments [7, 38]. Each annealing history is referred to by the temperature of its first plateau.

The figure of merit analysed in this section is the helium fractional release. Figure B.2 reports the results obtained with the updated version of SCIANTIX. The plots are identical to the ones obtained by [7], shown in Figure B.3.

It proves that the modified version of SCIANTIX does not affect the previous works. The new code is able to deal with pure helium bubbles as well as with mixed bubbles. This conclusion was expected, even if not obvious, since the new coupled path does not interfere with the separated paths.
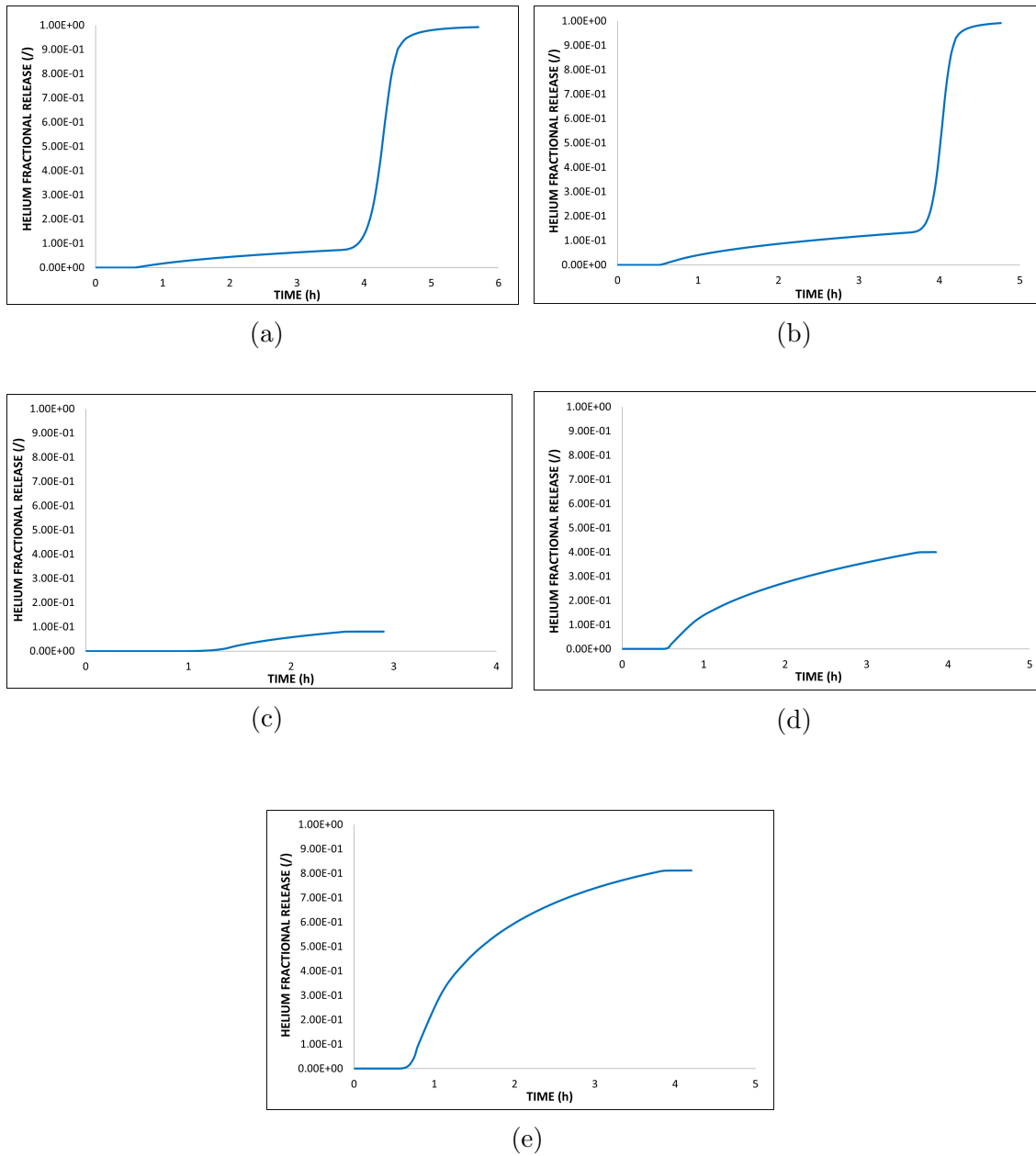
(a)

(b)

(c)

(d)

(e)

Figure B.2: Simulations performed after the update of SCIANTIX. Each subfigure represents the helium fractional release corresponding to an annealing history, respectively: (a) 1320K , (b) 1400 K, (c) 1400 K, (d) 1600 K and (e) 1800 K.

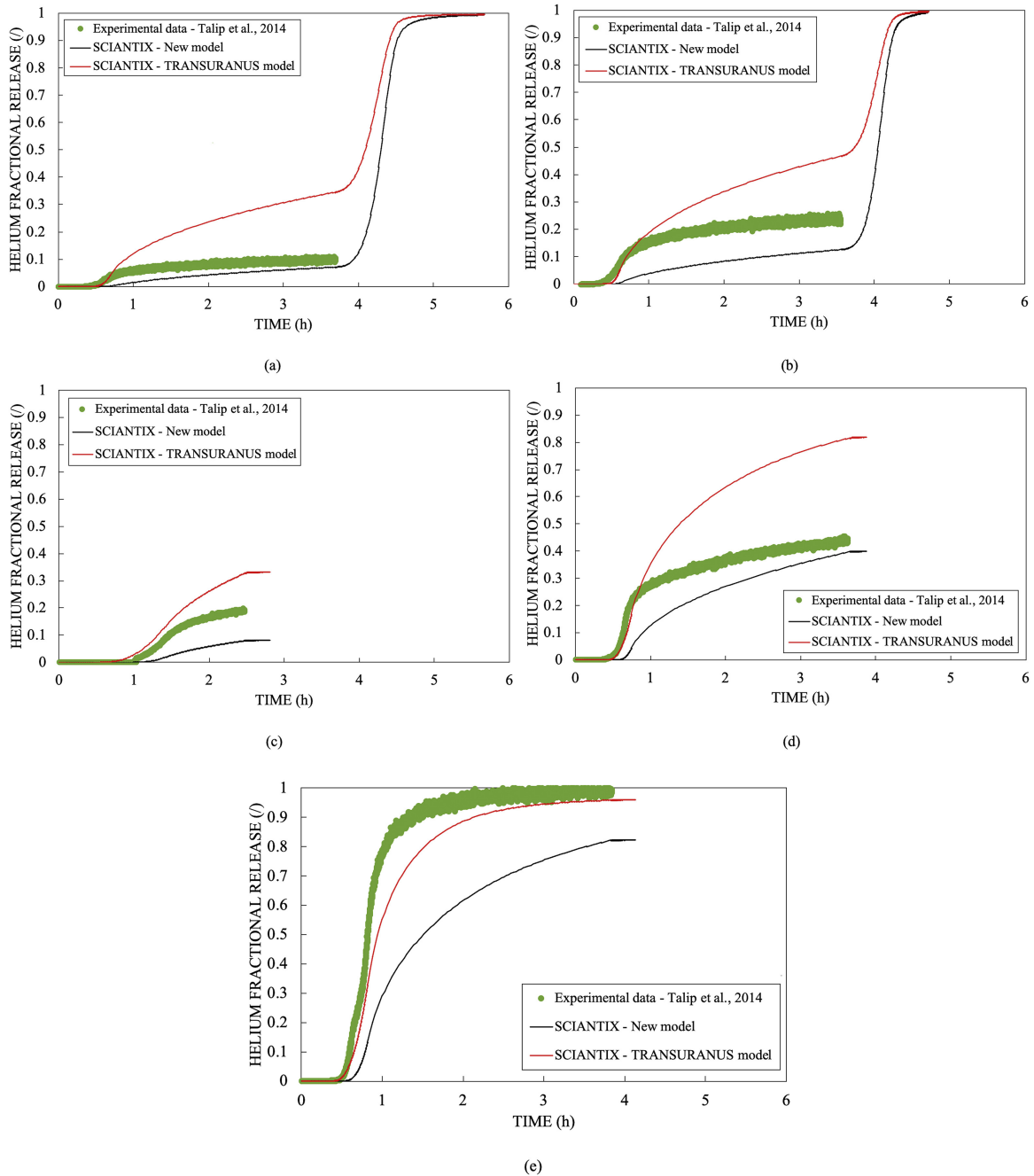Figure B.3: Helium fractional release from the work of [7] with the helium model indicated as SCIANTIX-New model. Each subfigure corresponds to an annealing history which is referred to by the temperature of its first plateau, respectively (a) 1320 K, (b) 1400 K, (c) 1400 K, (d) 1600 K, and (e) 1800 K. The additional results reported in the plots are not necessary for the purpose of this section.

Bibliography

[1] C Baker. "The fission gas bubble distribution in uranium dioxide from high temperature irradiated SGHWR fuel pins". In: *Journal of Nuclear Materials* 66.3 (1977), pp. 283–291.

[2] Jack Belle. *Uranium dioxide: properties and nuclear applications*. Vol. 4. Naval Reactors, Division of Reactor Development, US Atomic Energy Commission, 1961.

[3] AH Booth. *A method of calculating fission gas diffusion from UO 2 fuel and its application to the X-2-f loop test*. Tech. rep. Atomic Energy of Canada Limited, 1957.

[4] Pietro Botazzoli. *Helium production and behaviour in LWR oxide nuclear fuels*. 2011.

[5] Norman F Carnahan and Kenneth E Starling. "Equation of state for nonattracting rigid spheres". In: *The Journal of chemical physics* 51.2 (1969), pp. 635–636.

[6] CF Clement and MH Wood. "The principles of nucleation theory relevant to the void swelling problem". In: *Journal of Nuclear Materials* 89.1 (1980), pp. 1–8.

[7] L Cognini et al. "Towards a physics-based description of intra-granular helium behaviour in oxide fuel for application in fuel performance codes". In: *Nuclear Engineering and Technology* (2020).

[8] Luana Cognini et al. "Helium solubility in oxide nuclear fuel: Derivation of new correlations for Henry's constant". In: *Nuclear Engineering and Design* 340 (2018), pp. 240–244.

[9] Jean-Yves Colle et al. "A mass spectrometry method for quantitative and kinetic analysis of gas release from nuclear materials and its application to helium desorption from UO2 and fission gas release from irradiated fuel". In: *Journal of Nuclear Science and Technology* 51.5 (2014), pp. 700–711.

[10] Ian Crossland. *Nuclear fuel cycle science and engineering*. Elsevier, 2012.

[11] RC Ewing, WJ Weber, and FW Clinard Jr. "Progression Nucl". In: *Energy* 29 (1995), p. 63.

[12] E Federici et al. "Helium production and behavior in nuclear oxide fuels during irradiation in LWR". In: *Proceedings of the 2007 LWR Fuel Performance Meeting/TopFuel 2007'Zero by 2010'*. 2007.

[13] M Fell and SM Murphy. "The nucleation and growth of gas bubbles in irradiated metals". In: *Journal of Nuclear Materials* 172.1 (1990), pp. 1–12.

[14] Frank S Ham. "Theory of diffusion-limited precipitation". In: *Journal of Physics and Chemistry of Solids* 6.4 (1958), pp. 335–351.

[15] Toshiaki Kogai. "Modelling of fission gas release and gaseous swelling of light water reactor fuels". In: *Journal of Nuclear Materials* 244.2 (1997), pp. 131–140.

[16] Pekka Lösönen. "On the behaviour of intragranular fission gas in UO2 fuel". In: *Journal of nuclear materials* 280.1 (2000), pp. 56–72.

[17] L Luzzi et al. "Helium diffusivity in oxide nuclear fuel: Critical data analysis and new correlations". In: *Nuclear Engineering and Design* 330 (2018), pp. 265–271.

[18] G Martin et al. "A NRA study of temperature and heavy ion irradiation effects on helium migration in sintered uranium dioxide". In: *Journal of nuclear materials* 357.1-3 (2006), pp. 198–205.

[19] G Martin et al. "Irradiation-induced heterogeneous nucleation in uranium dioxide". In: *Physics Letters A* 374.30 (2010), pp. 3038–3041.

[20] Hj Matzke. "Gas release mechanisms in UO2—a critical review". In: *Radiation Effects* 53.3-4 (1980), pp. 219–242.

[21] E Maugeri et al. "Helium solubility and behaviour in uranium dioxide". In: *Journal of nuclear materials* 385.2 (2009), pp. 461–466.

[22] Kunihisa Nakajima et al. "The solubility and diffusion coefficient of helium in uranium dioxide". In: *Journal of nuclear materials* 419.1-3 (2011), pp. 272–280.

[23] Takehiko Nakamura et al. "Fission gas induced cladding deformation of LWR fuel rods under reactivity initiated accident conditions". In: *Journal of nuclear science and technology* 33.12 (1996), pp. 924–935.

[24] RS Nelson. "The influence of irradiation on the nucleation of gas bubbles in reactor fuels". In: *Journal of Nuclear Materials* 25.2 (1968), pp. 227–232.

[25] Donald R Olander. "Fundamental aspects of nuclear reactor fuel elements". In: *TID* 26711 (1976), P1.

[26] Donald R Olander. "Theory of helium dissolution in uranium dioxide. II. Helium solubility". In: *The Journal of Chemical Physics* 43.3 (1965), pp. 785–788.

[27] DR Olander and D Wongsawaeng. "Re-solution of fission gas–A review: Part I. Intragranular bubbles". In: *Journal of nuclear materials* 354.1-3 (2006), pp. 94–109.

[28] Giovanni Pastore et al. "Physics-based modelling of fission gas swelling and release in UO2 applied to integral fuel rod analysis". In: *Nuclear Engineering and Design* 256 (2013), pp. 75–86.

[29] D Pizzocri, T Barani, and L Luzzi. "SCIANTIX: A new open source multi-scale code for fission gas behaviour modelling designed for nuclear fuel performance codes". In: *Journal of Nuclear Materials* 532 (2020), p. 152042.

[30] D Pizzocri et al. "A model describing intra-granular fission gas behaviour in oxide fuel for advanced engineering tools". In: *Journal of Nuclear Materials* 502 (2018), pp. 323–330.

[31] D Pizzocri et al. "D6. 1–Review of available models and progress on the sub-models dealing with the intra-and intergranular inert gas behaviour". In: (2019).

[32] Firooz Rufeh. "Solubility of helium in uranium dioxide (M.Sc. thesis)". In: (1964).

[33] Firooz Rufeh, Donald R Olander, and Thomas H Pigford. "The solubility of helium in uranium dioxide". In: *Nuclear science and engineering* 23.4 (1965), pp. 335–338.

[34] MV Speight. "A calculation on the migration of fission gas in material exhibiting precipitation and re-solution of gas atoms under irradiation". In: *Nuclear Science and Engineering* 37.2 (1969), pp. 180–185.

[35] J Spino et al. "Matrix swelling rate and cavity volume balance of UO2 fuels at high burn-up". In: *Journal of Nuclear Materials* 346.2-3 (2005), pp. 131–144.

[36] Pei Sung. "Equilibrium solubility and diffusivity of helium in single-crystal uranium dioxide." In: (1967).

[37] D. Pizzocri T. Barani L. Luzzi. *SCIANTIX code, Online Repos.[Online]. Available.* URL: https://gitlab.com/poliminrg/sciantix. Accessed: 04-Oct-2019.

[38] Z Talip et al. "Thermal diffusion of helium in 238Pu-doped UO2". In: *Journal of nuclear materials* 445.1-3 (2014), pp. 117–127.

[39] JA Turnbull. "The distribution of intragranular fission gas bubbles in UO2 during irradiation". In: *Journal of Nuclear Materials* 38.2 (1971), pp. 203–212.

[40] JA Turnbull, RJ White, and C Wise. *The diffusion coefficient for fission gas atoms in uranium dioxide.* Tech. rep. 1989.

[41] JA Turnbull et al. "The diffusion coefficients of gaseous and volatile species during the irradiation of uranium dioxide". In: *Journal of Nuclear Materials* 107.2-3 (1982), pp. 168–184.

[42] Laurent Van Brutzel and Alain Chartier. "A new equation of state for helium nanobubbles embedded in UO2 matrix calculated via molecular dynamics simulations". In: *Journal of Nuclear Materials* 518 (2019), pp. 431–439.

[43] P Van Uffelen et al. "On the relations between the fission gas behaviour and the pellet-cladding mechanical interaction in LWR fuel rods". In: *Pellet-Clad Interaction in Water Reactor Fuels* (2004).

[44] Paul Van Uffelen. "Contribution to the modelling of fission gas release in light water reactor fuel". In: *PhD report* (2002).

[45] Paul Van Uffelen et al. "A review of fuel performance modelling". In: *Journal of Nuclear Materials* 516.INL/JOU-18-45934-Rev000 (2018).

[46] Paul Van Uffelen et al. "Analysis of reactor fuel rod behavior". In: *Handbook of nuclear engineering*. 2010.

[47] L Verma, L Noirot, and P Maugis. "Modelling intra-granular bubble movement and fission gas release during post-irradiation annealing of UO2 using a meso-scale and spatialized approach". In: *Journal of Nuclear Materials* 528 (2020), p. 151874.

[48] MS Veshchunov. "On the theory of fission gas bubble evolution in irradiated UO2 fuel". In: *Journal of nuclear materials* 277.1 (2000), pp. 67–81.

[49] RJ White and MO Tucker. "A new fission-gas release model". In: *Journal of Nuclear Materials* 118.1 (1983), pp. 1–38.

[50] Rodney J White. "The development of grain-face porosity in irradiated oxide fuel". In: *Journal of Nuclear Materials* 325.1 (2004), pp. 61–77.

[51] Thierry Wiss et al. "Evolution of spent nuclear fuel in dry storage conditions for millennia and beyond". In: *Journal of Nuclear Materials* 451.1-3 (2014), pp. 198–206.